British Geological Survey

Developing a UK new ground electric field model for SWIMMR N4 (SAGE): Interim Report

Multihazard and Resilience Programme

Open Report OR/22/067

BRITISH GEOLOGICAL SURVEY

MULTIHAZARD AND RESILIENCE PROGRAMME

COMMISSIONED REPORT OR/22/067

Developing a UK new ground electric field model for SWIMMR N4 (SAGE): Interim Report

J. Huebert, E. Eaton and C.D. Beggan

Science editor

A.W.P. Thomson

Keywords

Conductivity modelling; magnetotelluric measurements; space weather hazard; SWIMMR.

Front cover

Magnetotelluric Instrument installation at Oxendale, Lake District, February 2022

Bibliographical reference

HUEBERT, J., EATON, E. and BEGGAN, C.D. Developing a UK new ground electric field model for SWIMMR N4 (SAGE): Interim Report. *British Geological Survey Commissioned Report*, OR/22/067. 43pp.

Edinburgh British Geological Survey 2022

BRITISH GEOLOGICAL SURVEY

The full range of our publications is available from BGS shops at Nottingham, Edinburgh, London and Cardiff (Welsh publications only) see contact details below or shop online at www.geologyshop.com

The London Information Office also maintains a reference collection of BGS publications, including maps, for consultation.

We publish an annual catalogue of our maps and other publications; this catalogue is available online or from any of the BGS shops.

The British Geological Survey carries out the geological survey of Great Britain and Northern Ireland (the latter as an agency service for the government of Northern Ireland), and of the surrounding continental shelf, as well as basic research projects. It also undertakes programmes of technical aid in geology in developing countries.

The British Geological Survey is a component body of UK Research and Innovation.

British Geological Survey offices

Nicker Hill, Keyworth,
Nottingham NG12 5GG
Tel 0115 936 3100

BGS Central Enquiries Desk
Tel 0115 936 3143
email enquiries@bgs.ac.uk

BGS Sales
Tel 0115 936 3241
email sales@bgs.ac.uk

The Lyell Centre, Research Avenue South,
Edinburgh EH14 4AP
Tel 0131 667 1000
email scotsales@bgs.ac.uk

Natural History Museum, Cromwell Road,
London SW7 5BD
Tel 020 7589 4090
Tel 020 7942 5344/45
email bgslondon@bgs.ac.uk

Cardiff University, Main Building, Park Place,
Cardiff CF10 3AT
Tel 029 2167 4280

Maclean Building, Crowmarsh Gifford,
Wallingford OX10 8BB
Tel 01491 838800

Geological Survey of Northern Ireland, Department of Enterprise, Trade & Investment, Dundonald House, Upper Newtownards Road, Ballymiscaw,
Belfast, BT4 3SB
Tel 01232 666595
www.bgs.ac.uk/gsni/

Natural Environment Research Council, Polaris House, North Star Avenue, Swindon SN2 1EU
Tel 01793 411500 Fax 01793 411501
www.nerc.ac.uk

UK Research and Innovation, Polaris House,
Swindon SN2 1FL
Tel 01793 444000
www.ukri.org

Website www.bgs.ac.uk
Shop online at www.geologyshop.com

Foreword

This document is an interim report from the British Geological Survey (BGS) for the joint NERC-STFC Space Weather Instrumentation, Measurement, Modelling and Risk (SWIMMR) – Activities in Ground Effects (SAGE) programme on the production of a new *ground electric field* model for the UK. The report details the pre-existing models available noting their limitations, and then describes the instrumentation, deployment, and measurement of the magnetotelluric campaign to collect new magnetic and geoelectric data at sites across the UK. These measurements will aid a full UK-wide representation of the geoelectric field for space weather purposes.

Acknowledgements

In addition to the authors, other BGS staff have contributed to the production of this report. We thank Eleanor Maume, now resigned, for her assistance at the beginning of the SAGE fieldwork programme. Helen Smith, Guanren Wang and Sarah Watson have provided field assistance on the deployments. Aideliz Montiel at the University of Edinburgh has also been helping with fieldwork as part of her PhD project. We thank Tom Martyn and Rob Lyon for supporting the project with technical assistance and for help with the deployment of the magnetotelluric instrumentation.

We thank our project partners Colin Hogg and Duygu Kiyan in the Dublin Institute of Advanced Studies (DIAS), Ireland for the loan of their broadband magnetotelluric instruments and support in maintaining them.

Finally, we thank the many landowners for their generosity in allowing the use of their land for the temporary deployment of the magnetotelluric systems.

Contents

FIGURES

TABLES

Summary

This interim report describes progress made to date in the SWIMMR N4 (SAGE) project regarding the update of geoelectric field modelling in Britain during magnetic storms.

We describe research efforts to understand how the present thin-sheet method of computing the geoelectric field from magnetic variation data compares to the measured field at the three UK observatories. We then examine how measured magnetotelluric (MT) impedances can be used to improve the modelled geoelectric field during space weather events.

Next, we describe the fieldwork campaign to collect new high quality magnetotelluric data in Britain. As of August 2022, BGS have collected magnetic and electric field measurements at 32 sites across England, southern Scotland, and Wales. Around 18 remain to be completed by March 2023.

We present results from all the sites collected thus far. The measurements have been used to compute MT impedances which demonstrate large variability attributed to the underlying geology across Britain. We use the new MT data to re-evaluate the geoelectric field during the September 2017 storm and find large differences, for example, in central Yorkshire the electric field estimates are about one-tenth the magnitude observed in Lincolnshire around 100 km distant.

In the future the MT measurements will be included in a new 3D model of the conductivity of Britain for space weather hazard purposes.

1 Introduction

During severe space weather events, the Earth's magnetic field can change rapidly with large variations in the order of thousands of nT at mid-latitudes (Rogers *et al.,* 2020; Thomson *et al*., 2011). The time variations of the externally-driven magnetic field induce geoelectric fields in the conductive ground, whose magnitude and spatial scale depend on the underlying electrical conductivity structure. For long period variations (tens to hundreds of seconds) in resistive geology, the skin-depth is large (100-1000 km) and the magnetic field generates a relatively large geoelectric field. Short period variations (less than 10 seconds) of the magnetic field in a conductive subsurface have shallow skin depths (0.1-1 km) and produce relatively weak geoelectric fields (e.g., Simpson & Bahr, 2021).

Strong geoelectric fields, which can be up to several tens of V/km in some locations (Love *et al.,* 2018), build up over large areas posing a hazard to certain types of modern technology. With widespread adoption of low-resistance grounded infrastructure, such as high voltage (HV) power networks, induced geoelectric fields can more readily equalize through the earthing points of these conductors. These quasi-steady DC currents are called Geomagnetically Induced Currents (GICs) and, though small in comparison to the load carried, are a threat to the safe and optimal operation of HV transformers (Boteler, 2006; Pulkkinen *et al*., 2012). A well-known example of damage from GICs is the failure of the Québec-Hydro network in March 1989 (Bolduc, 2002; Boteler, 2019). The present-day cost of a similar widespread and long-lasting power outage could be of the order of tens of billions of US dollars per day (Oughton *et al.*, 2018).

Geomagnetically induced currents are therefore recognised as a potential hazard to electrical power transmission systems across the world, particularly at higher latitudes or in regions with lengthy high-voltage transmission lines. The first step in understanding this hazard is to quantify the induced geoelectric (or telluric) field at the Earth's surface. Unfortunately, long-term measurements of the geoelectric field are rare and are only available at a few locations around the world including Hungary, Japan, the USA and the UK.

Hence, most hazard assessment relies on geoelectric field modelling based on measurements from magnetotelluric surveys and detailed computationally intensive 3D conductivity modelling (e.g., Rosenqvist *et al.,* 2022). Magnetotellurics is a wide-spread method to image the subsurface electrical conductivity (or its inverse, the electrical resistivity) in varying scales, from shallow subsurface to crustal targets and global induction studies. MT has been used intensively in mineral exploration, geothermal and environmental surveys and to investigate tectonic and volcanic settings but such datasets are often commercial and hard to access.

Only recently it was realized that MT data over larger regional scales can be used to help characterize space weather impact on ground infrastructure through modelling of the ground electric field during geomagnetic active times, and that there is therefore a need to collect new and reuse older and legacy data (Ayala *et al.*, 2022). There are efforts to encourage sharing of MT data in a similar way to that of seismic and geomagnetic data, but these have been slow due to the generally more restricted use of MT data.

In the absence of large MT datasets, many initial attempts to characterise the ground electrical conductivity have involved synthetic models based on geologic data and considerations. In the UK, a thin-sheet conductance model of the upper 3 km has been developed over the past two decades (Beamish, 2013; McKay, 2003). It is based on airborne electromagnetic (EM) data and laboratory measurements of electrical conductivity. With these models, regional electrical fields can be computed using the thin-sheet approach first conceived by Vasseur and Weidelt (1977), albeit with relatively large uncertainties (Beggan, 2015).

The present BGS capability in geoelectric field modelling uses the measured changes of the Earth’s magnetic field at the three UK observatories (Lerwick, Eskdalemuir and Hartland) as input. In combination with the thin-sheet conductivity model and an underlying 1D model of electrical conductivity of the lithosphere, we can produce time varying estimates of the

geoelectric field at a 10 km resolution across the UK (see Figure 1 for an example). This method has the advantage of being computationally fast, but it is known to generally underestimate the magnitude of the geoelectric field when compared to measured values (Beggan *et al.* 2021) and we will show below that in many locations in the UK it is not very accurate.

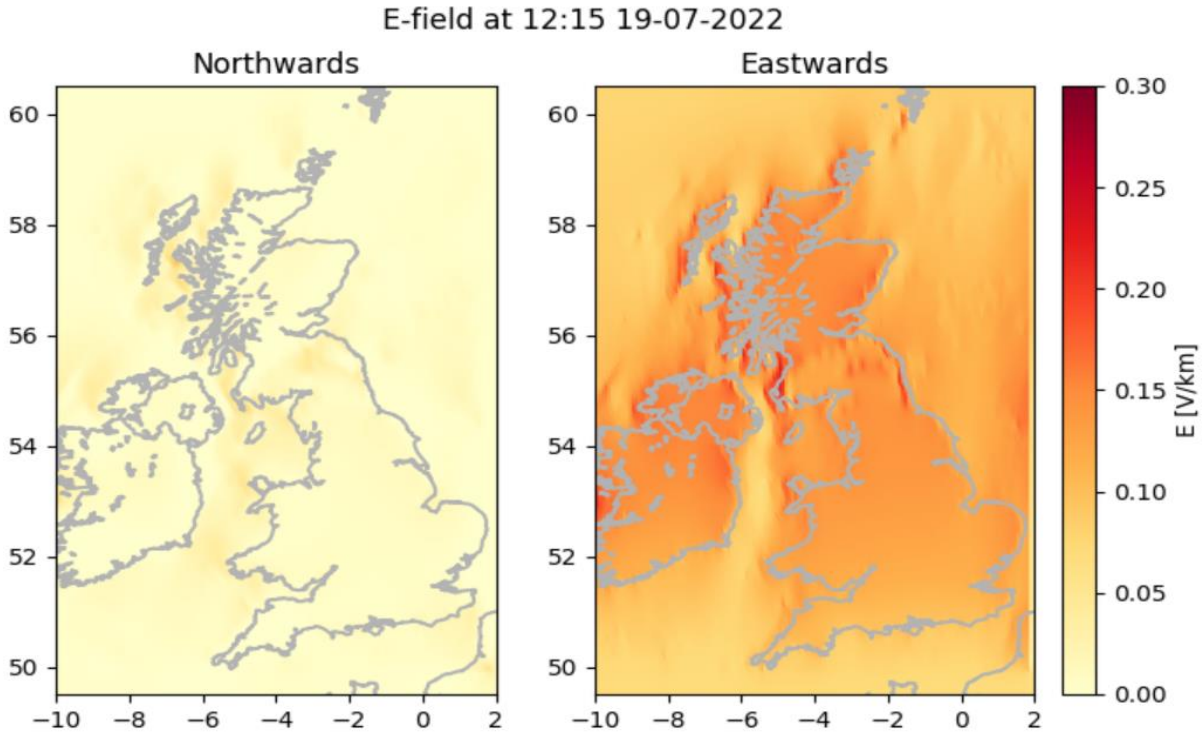

Figure 1: Modelled geoelectric fields using the BGS thin-sheet model for a quiet period on 19-Jul-2022: (left) geoelectric field in the Ex (northward) component and (right) Ey (eastwards) component.

As part of the NERC-STFC funded Space Weather Instrumentation, Measurement, Modelling and Risk (SWIMMR) programme, one major objective in the N4 SWIMMR Activities in Ground Effects (SAGE) project is to substantially improve existing geoelectric field modelling capability. We achieve this by: (i) making new magnetotelluric measurements for space weather purposes in England and Wales to supplement existing MT data; (ii) producing a new and more accurate ground electric field model of the UK and Ireland; and (iii) implementing the new modelling capability for real-time now-cast and forecast of the geoelectric field to allow the computation of GICs in the UK high voltage power system, high pressure pipeline network and rail systems.

The project was scheduled to begin in September 2020, but fieldwork to collect new MT data across England and Wales suffered from a six month delay due to travel restrictions during the Covid-19 pandemic in 2020. However, once all new MT data are collected it is anticipated that a new full 3D model of electrical conductivity below the British Isles can be constructed. A PhD project in conjunction with University of Edinburgh to help achieve this is also now in progress.

The report presented here outlines the initial work by BGS to meet the stated goals and presents methodology and results obtained so far (August 2022). In section 2 we describe the existing data and models, their origin and suitability for space weather forecasting. Section 3 describes the (presently on-going) magnetotelluric field campaign of 2021 and 2022 and a quick review of existing legacy MT data. In Section 4 we discuss and interpret some initial results of improved geoelectric field modelling and will be outlining the next steps in developing operational geoelectric field models for now- and forecasting of space weather impact on ground-based structures.

2 Modelling the Ground Electric Field for Space Weather Impact Assessment

Time-varying electric and magnetic fields occur naturally in the ground and induce each other as expressed through Maxwell's equations. The ground electric field (GEF) during geomagnetic storms is induced via the disturbed geomagnetic field and is also directly dependent on the ground electrical conductivity. During storm times, it varies much more laterally in comparison with the magnetic field because electrical charge carriers are very unevenly distributed in the subsurface. The ability to transport electric current in rocks is captured in the bulk electrical conductivity (resistivity). Conductivity is a wide-ranging rock parameter and depends mostly on the composition, pore space and fluid content of the rocks. For example, a porous fluid-saturated sandstone is a much better conductor than a dense young granite. The best electrical conductors in the context of geology are metals, melts and graphite.

Ground electric fields are generally quite small (in the range of mV/km) and can be measured via the potential difference between two metallic electrodes. For longer term measurements, non-polarizable electrodes are needed to avoid the build-up of charges due to electrochemical reactions.

To characterize the electric field over an area as large as the British Isles in real-time, we would need a large number (>50) of instruments measuring the geoelectric field. However, permanent deployment of such equipment is expensive and needs a large amount of resource to quality-check and maintain. In the UK, the ground electric field is currently monitored at three sites (the GB geomagnetic observatories in Lerwick, Eskdalemuir and Hartland) and the data collected there is described below. The sparse direct observations of the electric field make it necessary to develop numerical models to in-fill the gaps between measurement locations.

There are several approaches for calculating the geoelectric field during geomagnetically active times (Kelbert, 2020). For GEF modelling in the UK, we will discuss three main approaches: (i) 2D maps of the electric field at the surface created from a thin-sheet conductance model of the British Isles (ii) models of the ground electric field derived using the MT impedance tensor at specific sites (iii) full 3D estimates of the electric field based on a 3D inversion model of electrical conductivity derived from MT measurements.

All models of the ground electric field are compared to direct measurements at our observatory sites and we make an assessment of the quality of the model and the practicality of each of the three approaches.

2.1 GEOELECTRIC FIELD MEASUREMENTS

For long-term measurements of the ground electric field, the voltage between two points in the ground is measured using a pair of non-polarising electrodes to minimise self-potential that would otherwise appear as noise in the recording of differential voltage data (and therefore contaminate the signal of interest). At each UK observatory a similar set of sensors and recording equipment are used. The electrodes are of the LEMI-701 type, manufactured at the Lviv Centre of Institute for Space Research, Ukraine (https://lemisensors.com/). These were chosen for their low noise and long-term stability. The LEMI-701 electrodes are set into a copper and copper-sulphate solution (Cu-$CuSO_4$). At the observatories, two pairs of electrodes are installed in small hand-dug pits at least 0.5 m deep and set in a clay-$CuSO_4$ mix aligned in geographical North-South and East-West directions, with a dipole length of between 66 m and 100 m. The electronics which provide filtering, analogue-to-digital conversion and sampling were designed in-house and are undergoing constant maintenance and improvement by the Geomagnetism engineering team.

Due to the generally challenging environments in the remote locations and the normal decay of the probes, maintaining continuous high-quality measurements has not been possible. Various redesigns of the systems over the years as well as damage from lightning or component failure have caused gaps or poor-quality data for analysing longer periods. This is in addition to drifts

caused by the degradation of the electronics and ground probes and occasional steps in the data. This illustrates some of the reasons why widescale permanent deployment would be difficult and expensive to maintain.

Figure 2 shows an example of (excellent quality) measurements of the horizontal component of the ground magnetic field (H) and the geoelectric field in the east-west (EW) and north-south (NS) components at the three UK observatories (LER: Lerwick; ESK: Eskdalemuir; HAD: Hartland). The geoelectric field is strongly correlated to the rate-of-change of the horizontal and so dB/dt is often used as a proxy for the geoelectric field; though we note that the correlation with dB/dt is a function of local conductivity and hence geology.

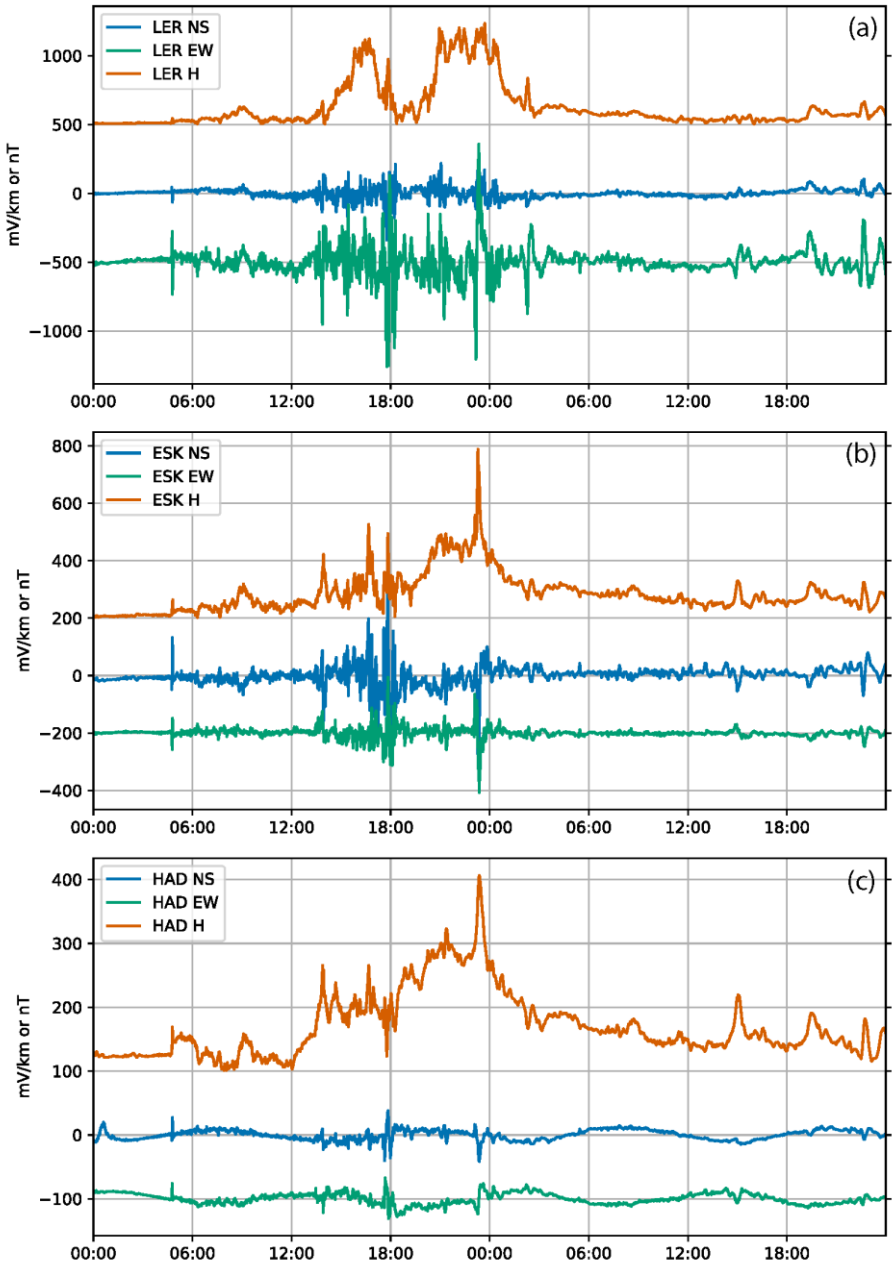

Figure 2: Horizontal magnetic field (H) and the two measured components (NS, EW) of the geoelectric field measurements at the three UK observatories (a) Lerwick, (b) Eskdalemuir and (c) Hartland, for the 17-March-2015. Time in UT.

2.2 THE EXISTING ELECTRICAL CONDUCTIVITY MODEL OF THE BRITISH ISLES

The UK is a geologically complex region with very old Precambrian metamorphic rocks in the northern part of the Highlands to more recent Cretaceous and Palaeocene sediments on the southern coast. To characterise these different regions, Beamish et al (2002) divided the deeper parts of the modelling space (that is, the British Isles) representing the middle and lower crust and the upper mantle into an assembly of six separate geological terranes, assigning different 1-D conductivity depth profiles to each area. The values in each terrane were based on legacy MT data inversions collected from the scientific literature.

Figure 3 shows the approximate geological extent of the underlying crustal terranes, typically bounded by large faults down to around 30 km. The long-period variations of the geoelectric field in each of these terranes is measurably different and produces strongly varying magnitudes (Beggan, 2015).

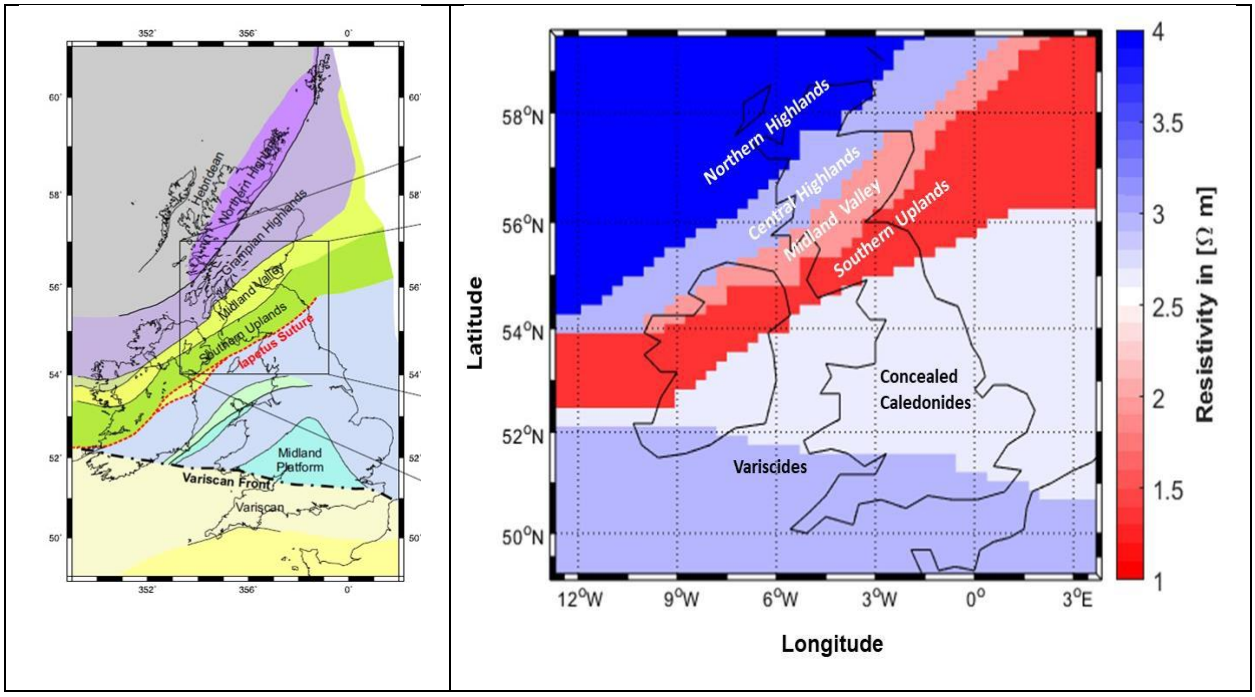

Figure 3: (left) Map of the inferred upper crustal geological terranes of Great Britain and Ireland after Beamish et al. (2002); (right) Representation of the six terranes in the BGS conductivity model.

The geoelectric field magnitude of the UK is also affected by the composition of the shallow geology, offshore sedimentation, and the bathymetry of surrounding seas. This shallow layer around 3-5 km deep, tends to redistribute the geoelectric field, generated deeper in the crust, along the edges of surface conductivity gradients. This enhances the geoelectric field along the coastline, for example, or at boundaries between strongly differing surface lithologies.

Beamish (2012) developed a series of models of the conductance of the UK to a depth of 3 km using airborne EM measurements from the Tellus project in Northern Ireland, Anglesey and Isle of Wight, which cover the vast majority of lithologies of the UK. These shallow conductivity measurements were linked to a GIS database of UK shallow bedrock electrical conductivity. Around 10% of the lithologies were missing, so laboratory measurements were used to complete the conductance map. He also included offshore sediments and bathymetry. Combining the thin-sheet conductance model and the 1D geologic terranes allows a continuous 2.5D representation of electrical conductivity under the British Isles. However, in the absence of more MT data that can represent the conductivity distribution at depth it was difficult to assess the accuracy of this synthetic model. Nonetheless it represented a state-of-the-art model of the conductivity at the time.

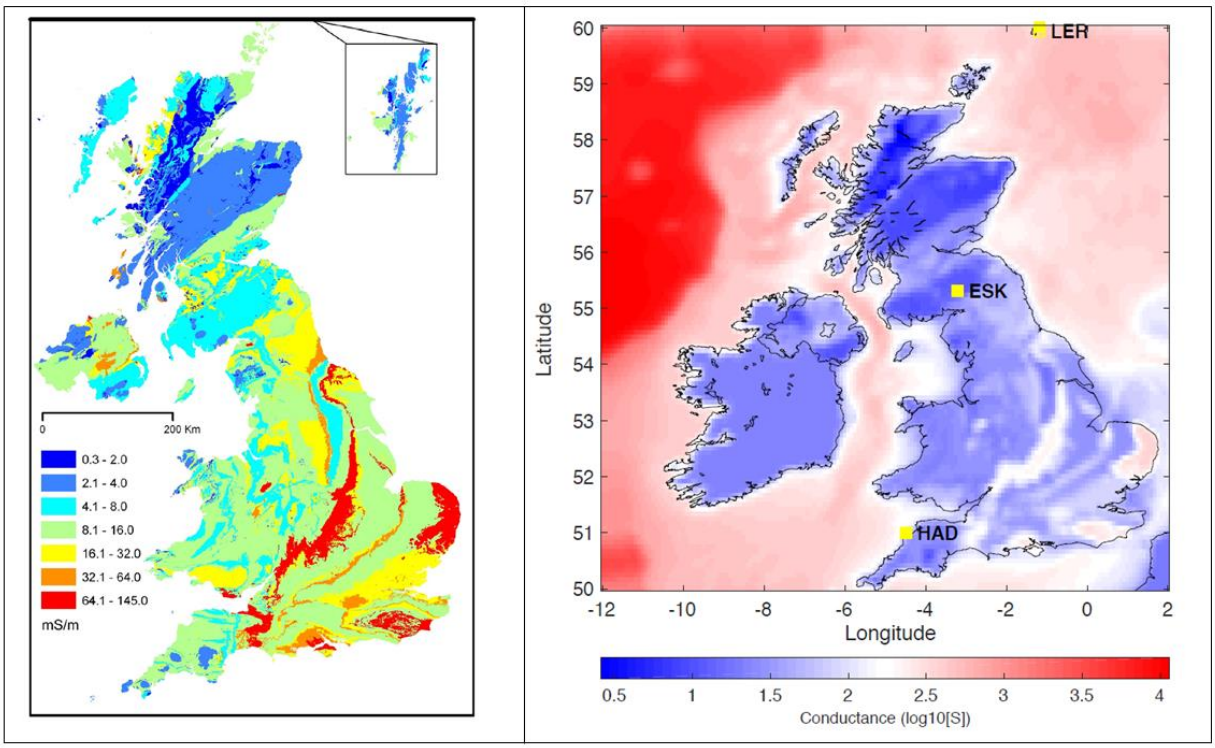

Figure 4: (left) Shallow bedrock electrical conductivity of the UK land areas, after Beamish (2012); (right) The derived conductance map of the upper 3 km of the British Isles including bathymetry and offshore sediments. BGS observatories marked as yellow squares.

2.3 THE THIN-SHEET METHOD

The peak period of the magnetic field variation that contains the signal caused by space weather is around 600 seconds (McKay, 2003) but the power of the geomagnetic field during geomagnetic storms is broadly spread between, with about 90% between 30 and 30,000 s (Campanya, 2019).

In the thin-sheet method, the geoelectric field is computed by convolving the derived conductance and underlying 1D conductivity with the magnetic field variation at a fixed period. The deeper 1D parts of the model induce the geoelectric field and the upper 2D part in a 10x10 km grid across the modelling area is treated as a thin sheet and redistributes the geoelectric field along gradients of conductivity.

The magnetic field across the British Isles is modelled using Spherical Elementary Currents (SECS, Amm, 1997) to incorporate the lateral inhomogeneity due to the influence of the electrojet that during geomagnetic active times can move southwards.

As an example, Figure 5 shows a model snapshot from the Halloween 2003 storm in the north-south (Ex) and east-west (Ey) directions for a period of 120 s. A value of around 1 V/km in the east-west direction of the geoelectric is modelled. The strongest effect on the geoelectric field is the location of the auroral electrojet, in this instant it lies across northern England as seen in the right panel (darker red regions). Therefore, the hazard posed by the geoelectric field is highly dynamic and constantly changing with time and location during a geomagnetic storm.

The second order effects on the magnitude of the geoelectric field are from the coastline and local subsurface and surface conductivity. It can also become locally enhanced; for example, Simpson et al. 2019 reported measured electric fields of up to 1.5 V/km in the Scottish Highlands during a moderately large storm in Sep 2017.

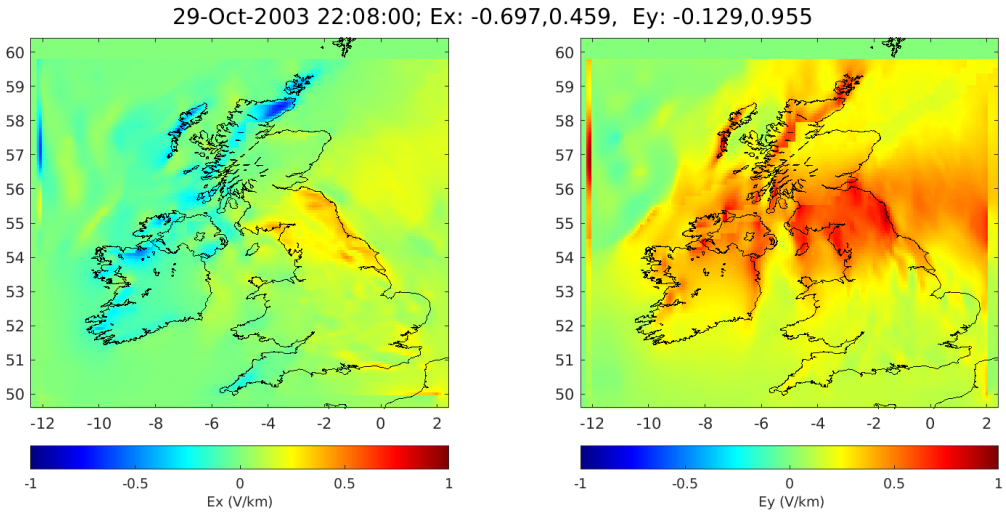

Figure 5: Snapshot of the geoelectric field for the Halloween 2003 storm at 22:08 UT on the 29th October. (left) Geoelectric field in the X (North) component; (right) Geoelectric field in the Y (East) component.

2.4 THE MAGNETOTELLURIC METHOD

The magnetotelluric (MT) method is a deep-sounding geophysical technique that uses the principles of electromagnetic induction to study the interior of the earth. By simultaneously recording the variations in the natural magnetic and electric field on the surface of the earth it is possible to derive models of underlying electrical conductivity. In practice, a magnetic sensor (for long period recordings a three-axial fluxgate magnetometer is used) samples the magnetic field in cartesian coordinates (x-north, y-east, z-downwards) every second. The horizontal electric field is measured with two dipoles. The recorded time series are filtered and transformed into frequency spectra which can then be used to derive the impedance tensor **Z**.

It is defined in the frequency domain ($\omega=2\pi/f$) and relates the variation of the magnetic field (**B**) to that of the electric field (**E**):

$$\mathbf{E}(\omega) = \frac{1}{\mu_0}\mathbf{Z}(\omega) \cdot \boldsymbol{B}(\omega)$$

where μ_0 is the permeability of free space. The **Z** tensor has four complex components:

$$\mathbf{Z} = \begin{pmatrix} Zxx & Zxy \\ Zyx & Zyy \end{pmatrix}$$

and is often displayed as apparent resistivity (a measure for the amplitude and the true resistivity if the subsurface is homogeneous) and phase curves for each component. These allow for a quick visual inspection of the magnitude and changes in conductivity in the subsurface with depth.

The inducing magnetic field is assumed to be spatially uniform, and **Z** is considered quasi-stationary (independent of when the recordings were performed) and only dependent on the local Earth response. Typically, MT recordings last from a few days to a couple of months. The length and quality of the data determines the frequency range of the computed transfer function, with the depth of investigation controlled by the skin depth of the EM waves.

Assuming a plane wave, the derived impedance tensor can then be used to estimate the induced geoelectric field in a wide frequency range at any other time when only magnetic field data are available (Campanya *et al.*, 2019; Hübert *et al.*, 2020; Lucas *et al.*, 2018).

As an example, at the UK geomagnetic observatories very long time series of both the magnetic and electric field are available (Beggan *et al.*, 2021; Baillie, 2020). Six months segments of one-

second cadence data from the magnetic and geoelectric instruments were therefore used to derive the impedances using the robust statistical algorithm of (Smirnov, 2003). From these measurements it is possible to estimate MT impedances for periods between 20 - 20,000 seconds (see Figure 6).

From the apparent resistivity curve, the Z_{xy} response of Lerwick (yellow open circles) is much lower and flatter than Eskdalemuir (blue open circles). This means that the ESK geoelectric field is much larger for very rapid changes of the magnetic field below 100 seconds compared to Lerwick, while they have equal response at longer periods around 10,000 seconds.

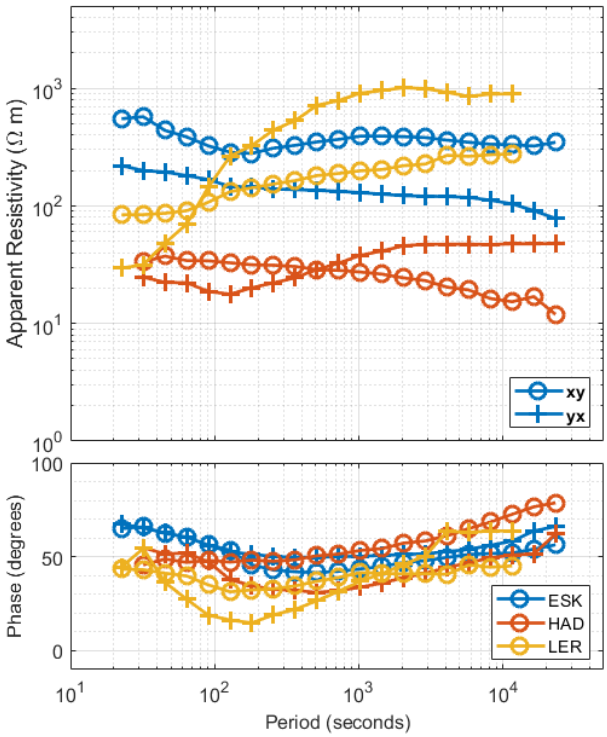

Figure 6: Main components (Z_{xy} and Z_{yx}) of the MT impedance tensor at all three UK observatories displayed as apparent resistivity (upper panel) and phase (lower panel) depending on period (a proxy for depth). Differences in curves reflect the varying underlying electrical resistivity structure across Britain.

2.5 GEOELECTRIC FIELD MODEL AND DATA COMPARISONS

The continuous measurements of the geoelectric field at the three UK observatories allow us to make a comparison between with the modelled values from the thin-sheet and impedance method and the data. Figure 7 shows the comparison of the geoelectric field measurements made at each geomagnetic observatory for the 17 March 2015 storm. The measured data in blue, the MT-derived values are in green and the thin-sheet modelled values are in orange. In Lerwick the geoelectric field variations reached over 1 V/km peak-to-peak around 18:00 UT in the east component, while it was around 50% smaller at Eskdalemuir with a peak-to-peak change of 500 mV/km. At the most southerly observatory, Hartland, the geoelectric field in this frequency band reaches around 50 mV/km peak-to-peak.

For the east component of the thin-sheet electric field at Lerwick, the magnitude is not well captured, though the match is better in the north component. The MT values are closer, though do not match the measured peak values. At Eskdalemuir, the thin-sheet comparison in phase and amplitude is much better in the north component compared to the east component, while in Hartland the magnitude is similar though the correlation is poorer.

Overall, this demonstrates that the thin-sheet model is not ideal and should be improved.

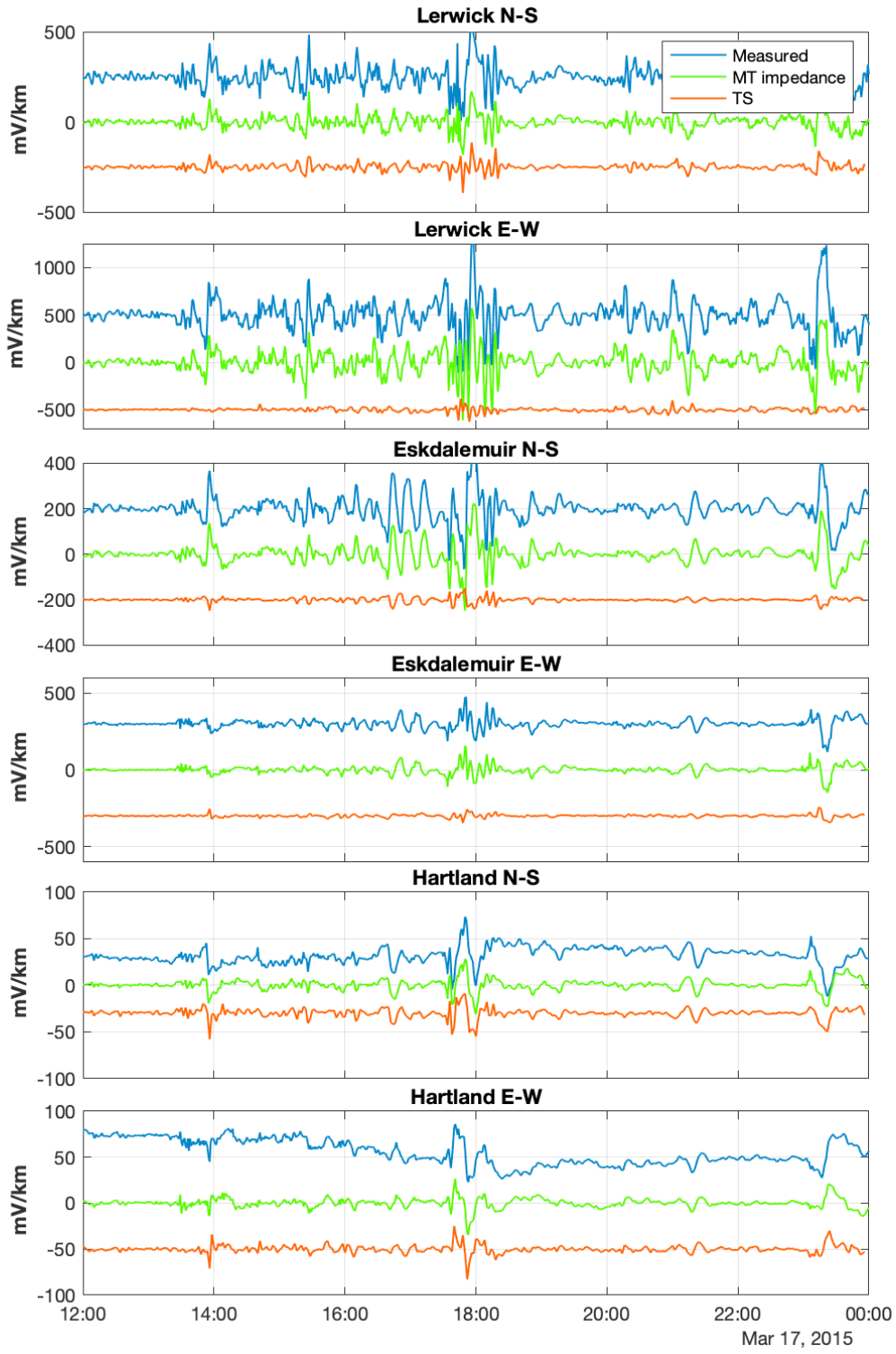

Figure 7: Comparison of the geoelectric field at the three UK observatories for 17 Mar 2015 from the measured values, thin-sheet (TS) model and MT-derived values.

2.6 COMPARISON OF GEOELECTRIC FIELD MODELLING USING THE THIN-SHEET AND THE MT-IMPEDANCE APPROACH

As seen in the previous subsection, electric fields at the three observatory sites calculated with the two presented modelling approaches – the thin-sheet model and the MT impedance model – differ strongly, with MT derived estimates better capturing the measured electrical field. In the absence of further MT data, we can attempt to show how the two modelling approaches would compare for the same underlying conductivity model. The computation of electric fields is numerically quite different for the methods, but the underlying physics should hold if the chosen electrical conductivity model is true or a good approximation.

The following paragraph contains a comparison of thin-sheet and MT impedance derived models using a model we will call the *cUK* model (combining the conductance thin sheet part with the geologic terranes in a piecewise 1-D layered lithospheric conductivity distribution). Note that this model is largely synthetic – based on independent inferences of but only few direct observations of conductivity at depth. This comparison will show how the thin-sheet approach (as it is computationally fast and covers the whole modelling region) is equivalent to the MT impedance method if the underlying conductivity models were to be based on a common dataset.

We first constructed a 3-D finite difference representation of the thin-sheet conductance and terranes model (Figure 8 and Figure 9). Using the forward solver from the ModEM code (Modular EM; Kelbert *et al.*, 2014), we compute synthetic MT impedance responses on a grid of locations in Great Britain. ModEM is a sophisticated inversion software package that is normally used to model MT responses and data to find models of electrical conductivity to image geologic targets. It computes electric and magnetic fields on a staggered grid covering the model area. The computation is implemented for parallel execution on high performance computing architecture to speed up the computation time which is substantial due to the large number of unknowns. The process is however not completely scalable, and the number of parallel processes is restricted to the number of frequencies of the data and the number of modes of the horizontally inclined EM field (in our case, two). For the inversion, response data of the model and measured data are evaluated for data fit and through an iterative process a model with optimized fit can be found. This process can take several days of computation time. For our short demonstration it was only necessary to compute the forward response for the combined conductance and terranes model once for the desired signal period (T = 600 s). We neglected topography but did test to include bathymetry, as conductive sea water can have a very strong effect on MT responses. However, due to the long-period signal of interest, the shallow sea water around the British Isles has only a small effect on the computed responses. The computed full 3-D MT responses were then compared with measured data at a few sites where MT data are available.

In detail, we projected the 2D conductance model from Beamish (2012) and 1D block model onto a rectangular grid (119 x 103 x 38 cells), converted conductance to resistivity (equally distributed between all cells in the upper 3 km). We then discretised the model space in horizontally 10x10 km blocks to match the resolution of the thin-sheet method. The cell sizes in the vertical direction were increased (starting at the surface with 14 m thickness, then increasing with a factor ~1.2 between each layer). We then computed forward impedance response at 235 locations sampling the land surface of Great Britain using ModEM for 25 periods 0.01-10,000s on the BGS High Performance Computing (HPC) cluster. The calculation took approximately 10 min per mode and frequency (on one HPC node).

The resulting MT impedances of the synthetic model were then compared to existing MT data at the UK geomagnetic observatories and for a legacy dataset measured in Dumfries, Scotland.

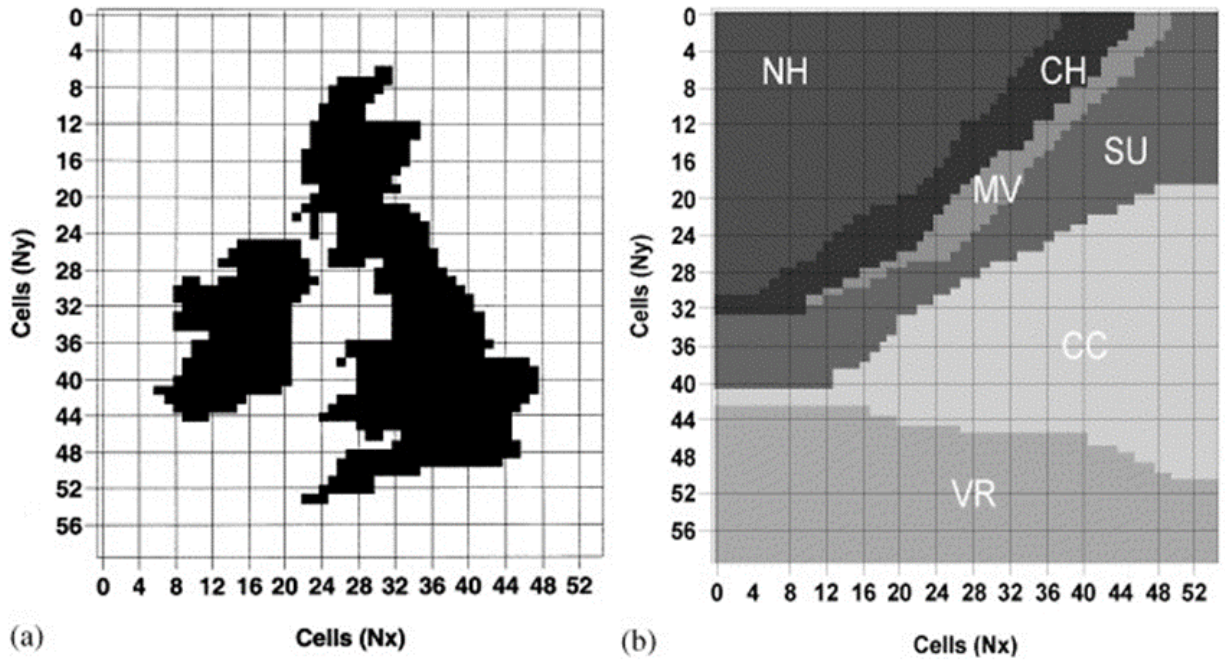

Figure 8: Terrane blocks after Beamish et al. (2003) after which we constructed the 1D conductivity model blocks.

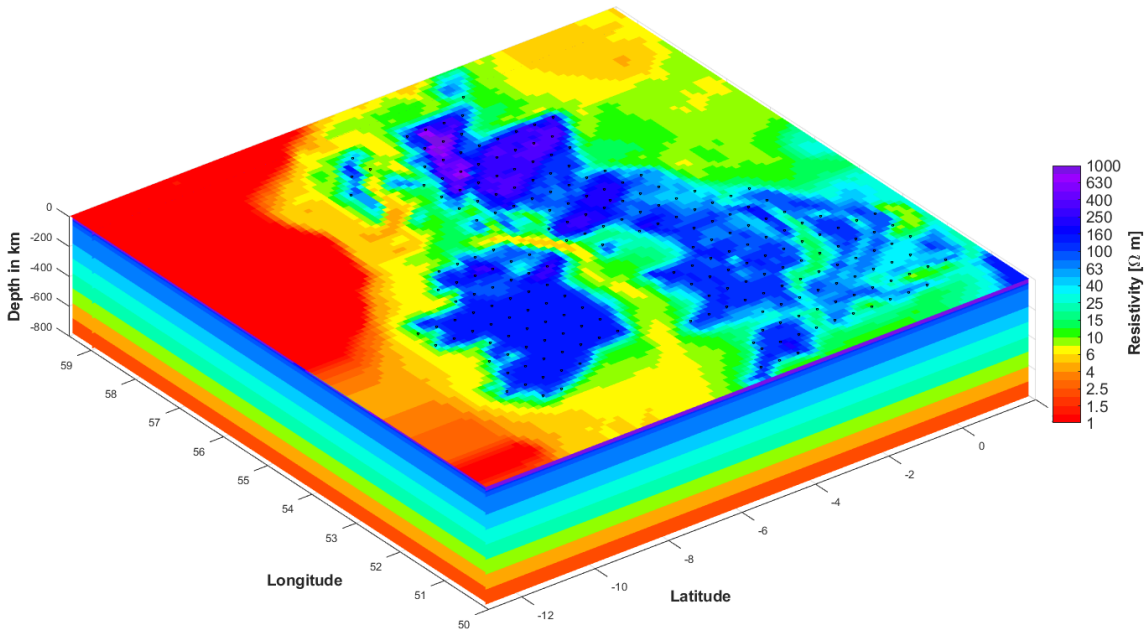

Figure 9: View of the 3-D finite difference representation of the thin-sheet conductance and underlying 1D lithosphere model. The model in this form is referred to as ‘cUK’ model. Black dots at the surface indicate locations where the MT impedance response is calculated.

From the comparison of synthetic and measured impedances we found that there are very noticeable difference. For ESK (Figure 10 and Figure 11), the Z_{xy} and Z_{xy} components of the impedance tensor show very different behaviour. The level of the apparent resistivity curves is much lower in the synthetic response. This indicates the real underlying conductivity structure (as represented in the measured impedance) has a completely different geometry (the strike direction) than the computed responses.

For HAD (Figure 12 and Figure 13), the comparison shows more similarities in the magnitude of apparent resistivity. In the measured data, there is a crossover between the two main components, whereas in the modelled response the curves are identical for all periods below 100 s which indicates an essentially 1D structure.

We included a comparison to a legacy broadband MT site MINN from Tauber *et al.* (2003) to investigate if the shallower parts of the model (as represented in the shorter period part of the impedances) are in agreement with measured data. The shorter periods in the data are represented by the conductance sheet that encompasses the lateral changes in the upper 3 km, including the coastline. In Figure 14 and Figure 15 the synthetic responses from cUK do not capture the strongly three-dimensional character of the measured impedances (as can be seen from the large amplitude of the diagonal components Z_{xx} and Z_{yy}).

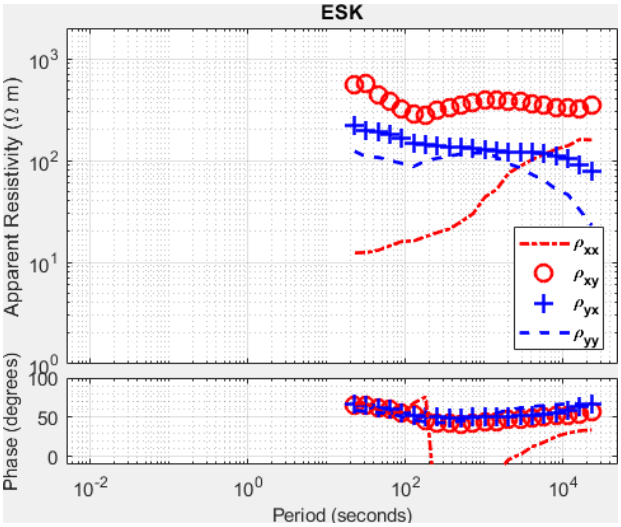

Figure 10: MT impedance at ESK derived from measurements. Note that only long-period data (> 10 s) is available.

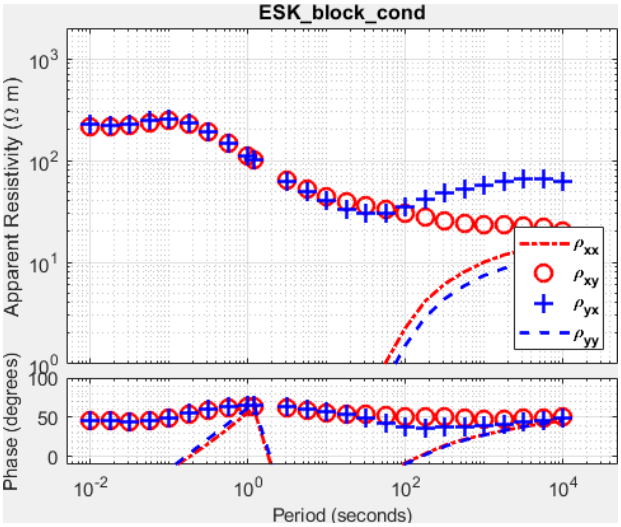

Figure 11: MT impedance at ESK computed from the cUK model which includes shorter periods (0.01-100 s) as well.

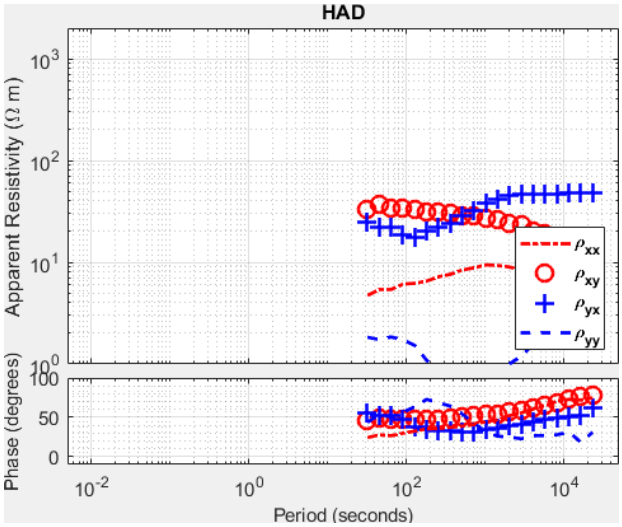

Figure 12: MT impedance at HAD derived from measurements. Note that only long-period data (> 10 s) is available.

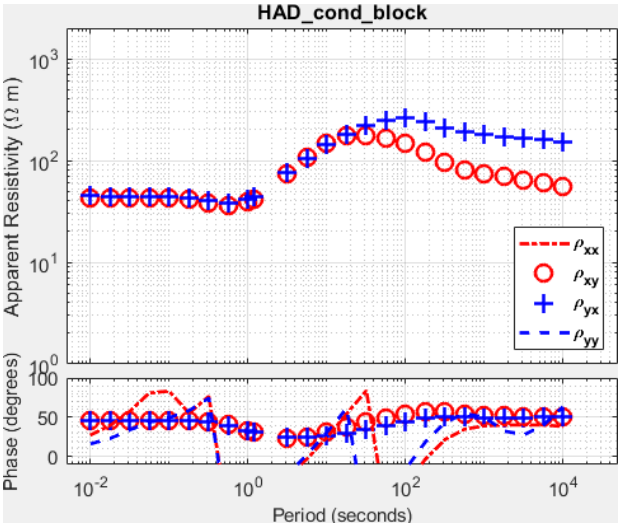

Figure 13: MT impedance at HAD computed from the cUK model.

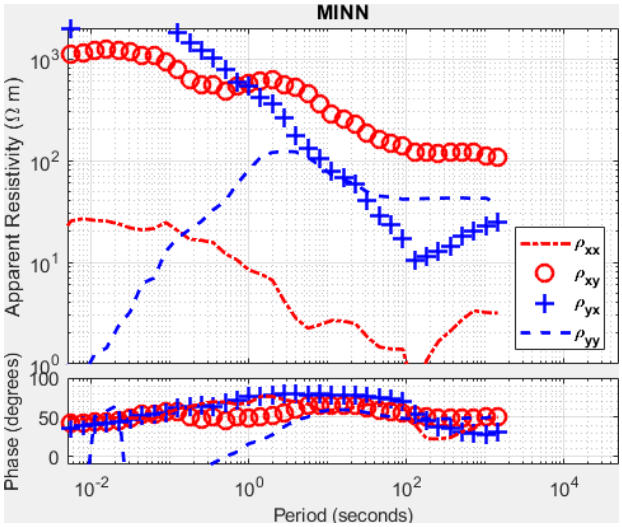

Figure 14: MT impedance from broadband site MINN, measured in southwest Scotland (Tauber *et al.*, 2003).

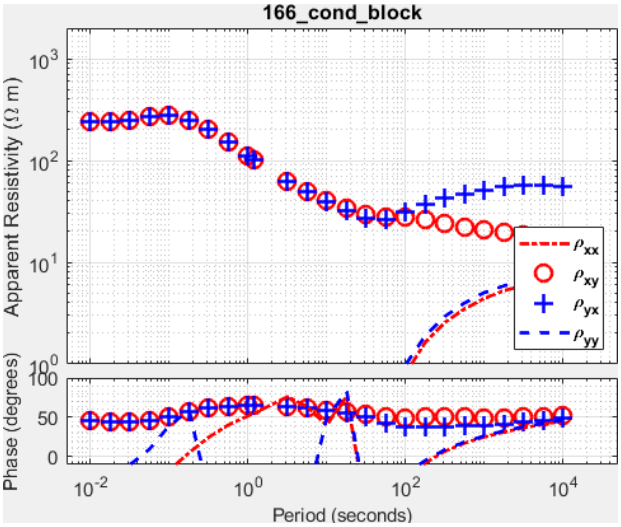

Figure 15: MT impedance at site MINN computed from cUK model.

In general, the comparison between the measured MT impedances and 3D modelled responses from the cUK model show a poor fit. This means that the synthetic cUK model does not fully represent the true three-dimensional underlying conductivity structure of the British Isles.

To investigate what consequences this has for the estimation of electric fields during geomagnetic storms, we performed further tests comparing the electric field predictions from the two methodologies. Using the synthetic impedance data from the cUK model provides a test case for future geoelectric field calculations once the MT field campaign has produced enough real data.

As an example, we computed electric fields during the September 2017 storm. Following several coronal mass ejections (CMEs) between 4-6 September 2017, the global Kp index rose to 8 during the night from the 7-8 September and then again around 18.00 UT on 8 September.

With the synthetic MT impedances from the cUK model we used the algorithm by (Campanya *et al.*, 2019) to compute electric fields during 7-9 September and compared to the solution of the thin-sheet model (Beggan *et al.*, 2021). Figure 16 and Figure 17 show similar, though not identical results for both methods. The Ex component is very similar in amplitude and spatial distribution, but in the Ey component there are lower amplitudes are modelled from the MT impedances in the southern part of Britain. There is more detail in the thin-sheet model due to the finer discretisation, but some smaller scale structures especially in the north of Scotland match well in both models. Equally when looking at the timeseries computed for the locations of the three observatories (Figure 18), the estimates from both methods look very similar. This suggests that both methods to derive electrical fields provide similar electric field estimates for the same electrical conductivity distribution. However, we know the thin sheet model tends to underestimate the geoelectric field in any case.

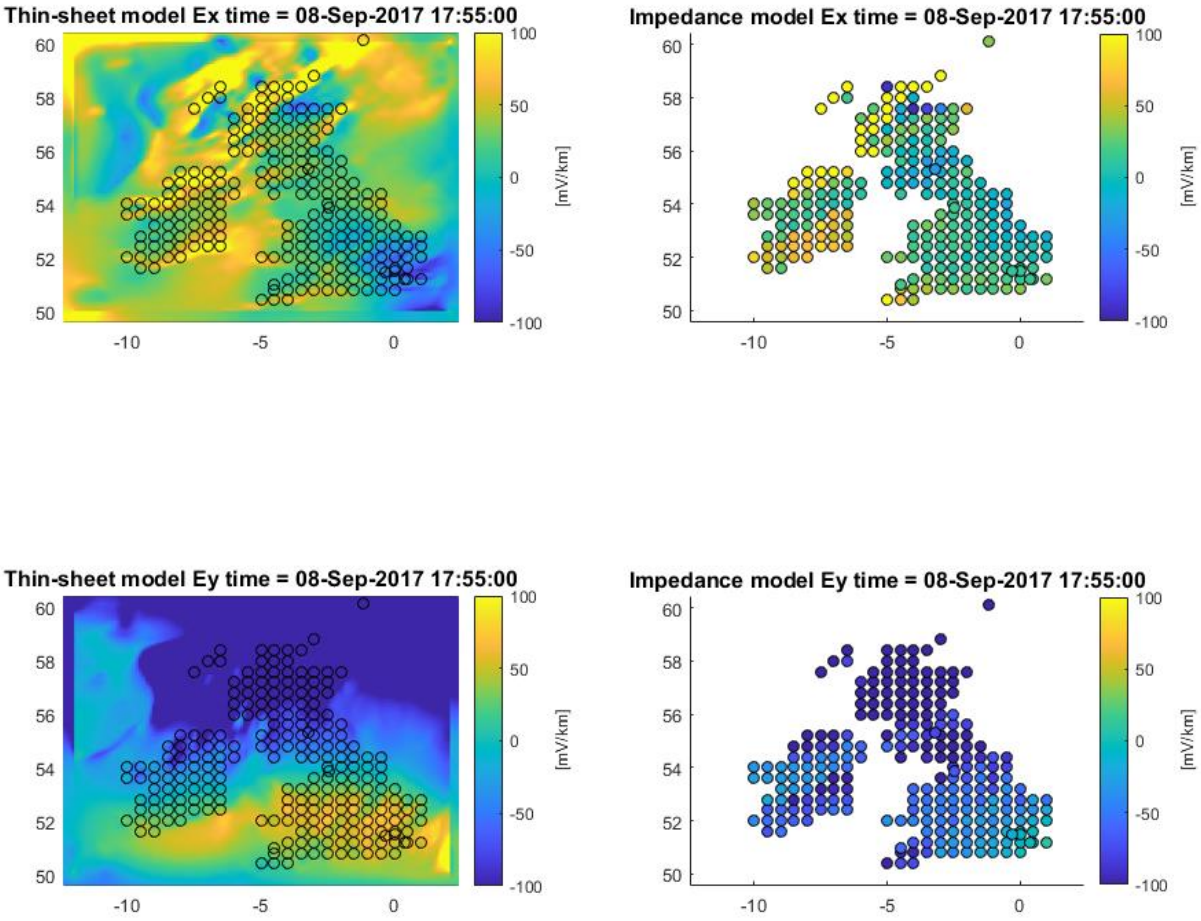

Figure 16: Time snapshot of the modelled geoelectric field in north-south (Ex) and east-west (Ey) direction on 8 September 2017, 17:55 UT, in the British Isles using the thin-sheet method (left panels) and MT impedance (right panels) derived fields using the cUK model.

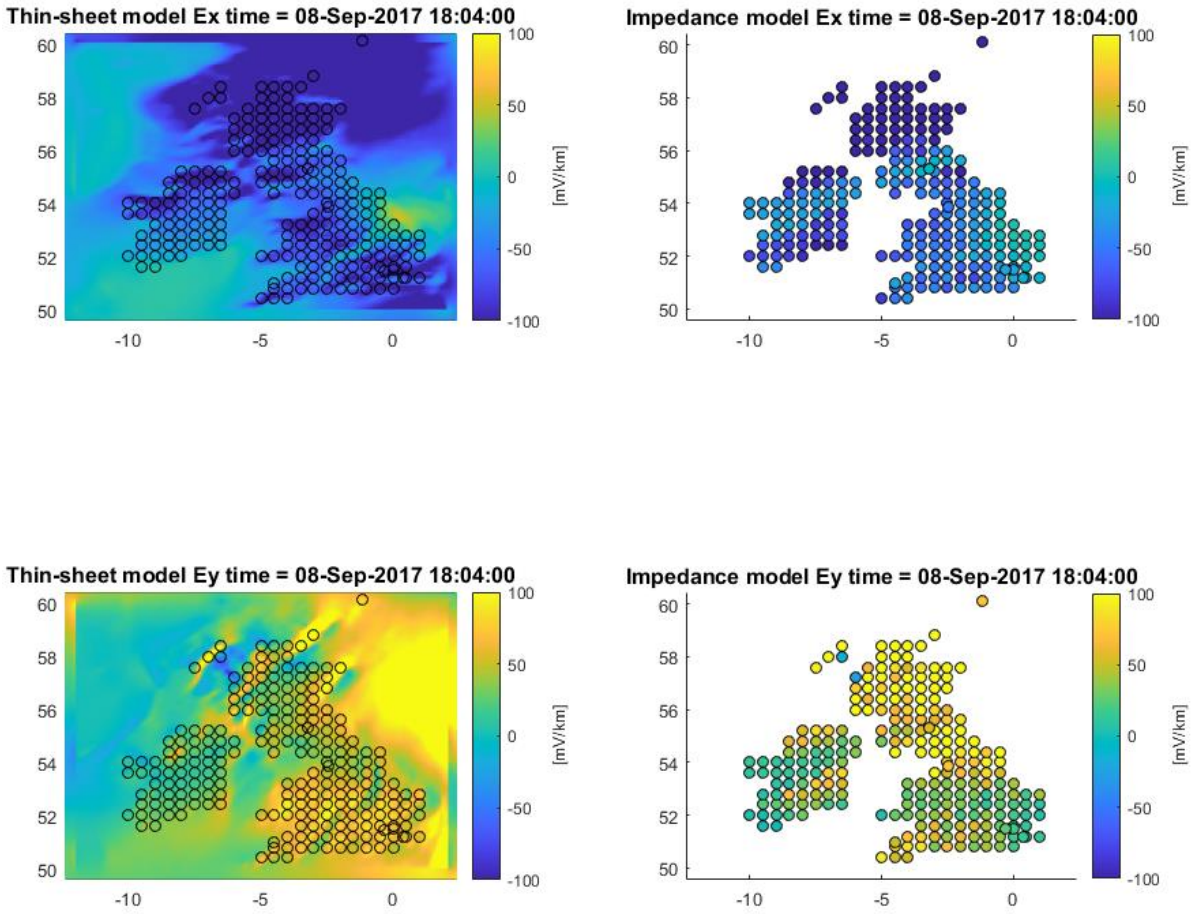

Figure 17: Time snapshot of the modelled geoelectric field in north-south (Ex) and east-west (Ey) direction on 8 September 2017, 18:04 UT, in the British Isles using the thin-sheet method (left panels) and MT impedance derived fields (right panels) using the cUK model.

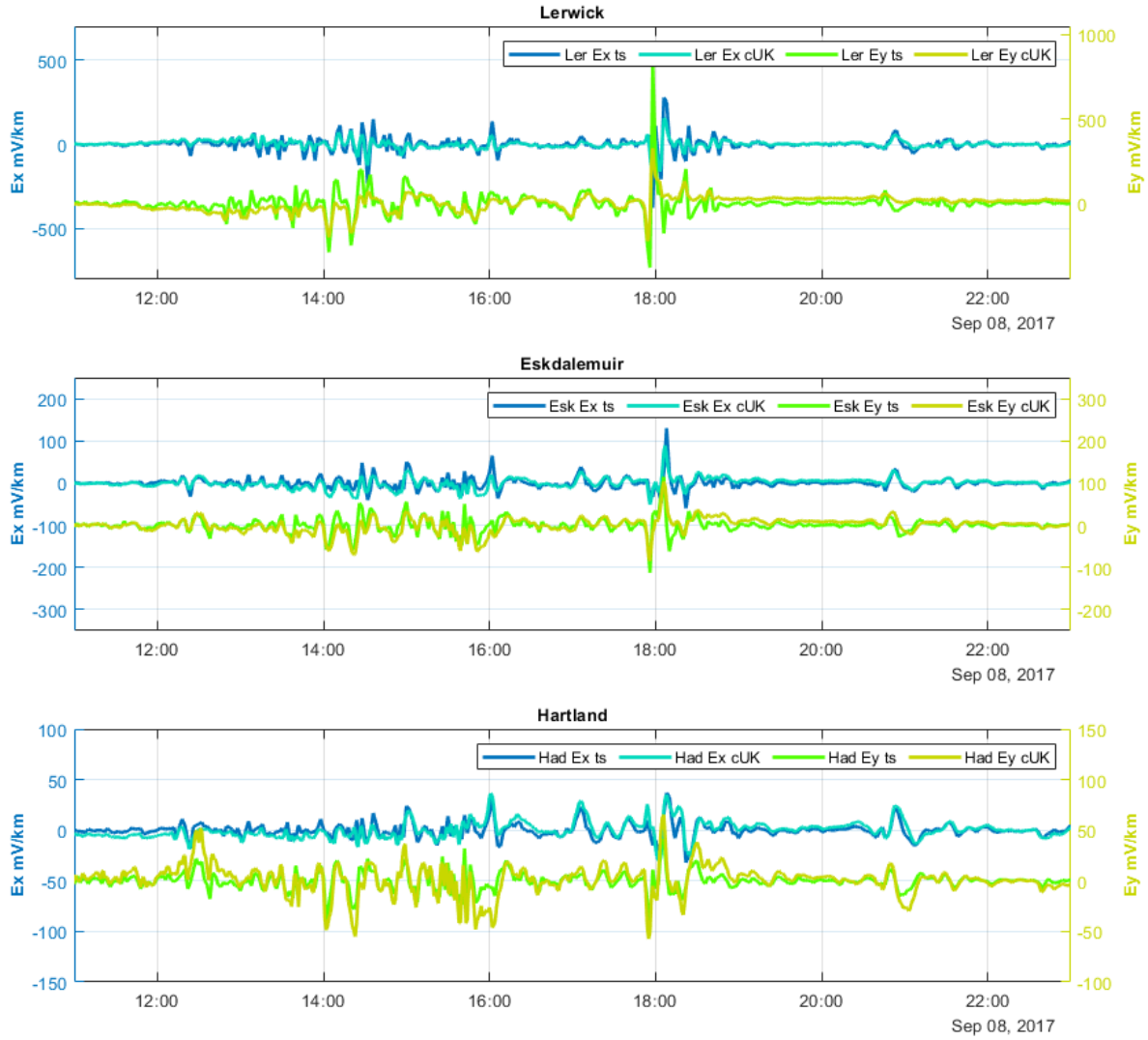

Figure 18: Thin-sheet vs. cUK impedance modelled electric fields for 8 September 2017 at UK observatory locations (LER – top panel, ESK – middle, HAD – lower panel). N-S directed fields are in blue, E-W directed fields in greenish colours.

3 New long-period Magnetotelluric Data

3.1 SAGE MT FIELD CAMPAIGN

Within the SWIMMR N4 SAGE project, BGS Geomagnetism have been tasked with the collection of new MT data across England and Wales at about 50 sites to complement existing data and equally sample Great Britain with approximately 50-70 km distance between sites, omitting large urban centres. Since MT is a passive method where signal-noise ratios are site-dependent, the careful selection of site locations is a priority. Ideally, the site is well away from all man-made electromagnetic signal sources like railway lines (>10 km), electric fences and power lines (>1 km), industry (>5 km), housing and generators (>2 km), similar to the recommendation for magnetic observations (Jankowski & Sucksdorff, 1997). Data collection for long-period signals takes about 4 weeks, so the site should be mostly undisturbed by people and livestock. All sensors are buried to about half a metre depth and well away from tree roots. Open skies for GPS signal and solar recharge are also necessary. As far as possible, we pre-selected sites using satellite images and open-source information on the location of railway and power lines. We thank all landowners and especially the National Trust for allowing land access.

3.2 INSTRUMENTATION AND INSTALLATION

For the field campaign, our project partners at the Dublin Institute for Advanced Studies provided four Lemi–417 magnetotelluric instruments (Figure 19) including electrodes via a loan agreement. Electric field cables, solar panels including regulators and deep-cycle batteries as well as enclosures were purchased by the SAGE project and assembled in-house. The typical layout of an MT site can be seen in Figure 20, and an installation can be seen in Figure 21. Special care is taken to ensure that the electric probes have good ground connection by watering them well. We checked the contact resistances between dipole pairs and if this was higher than >10 kΩm, electrodes were replaced. Higher contact resistances generally signify degradation of the probes due to leaking fluid and this can lead to higher noise levels and jumps in the self-potential. The magnetometer is aligned to magnetic East by manual rotation, minimizing the By component. Lemi magnetometers are watertight and quite robust with regard to temperature variations.

All cables are buried in shallow trenches to avoid damage from weather or livestock. The MT data are recorded in a Lemi-specific binary format in five separate channels (Ex, Ey, Bx, By and Bz). Information from temperature and battery life are recorded as well. The data can then be converted into ASCII format and subsequently processed to compute the impedances. We check data collection at each installation one day after installation to make sure that everything is recording correctly and to ensure data quality are sufficient.

Due to the travel restrictions in relation to the Covid-19 pandemic, the start of the field campaign was delayed from October 2020 to April 2021. However, a no-cost extension of six months by both NERC and DIAS for the instrument loan until March 2023 will allow us to complete the data collection as anticipated.

MT data collection follows a roll-on approach with continuous deployment of the four systems in use. We installed on average two to three sites each month (see Figure 22). Some initial instrumental problems in Spring 2021 required the replacement of two Lemi units. The instruments were transported back to Ireland and then to the manufacturer in Ukraine for a software update before coming back to BGS. An additional software update was performed in August 2022 by BGS personnel.

Figure 19: Lemi 417 magnetotelluric station components. From left to right: Electrodes, GPS antenna, fluxgate magnetometer, data recording unit, electric field interface

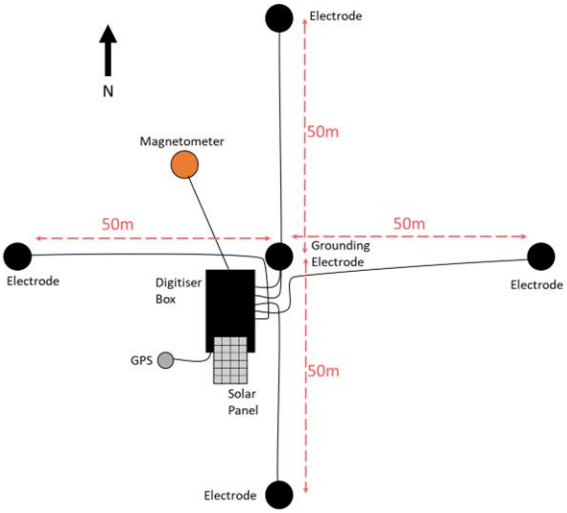

Figure 20: Map view of layout of LMT site.

Figure 21: MT installation NY20 in the Lake District. All cables are buried to avoid interference from livestock.

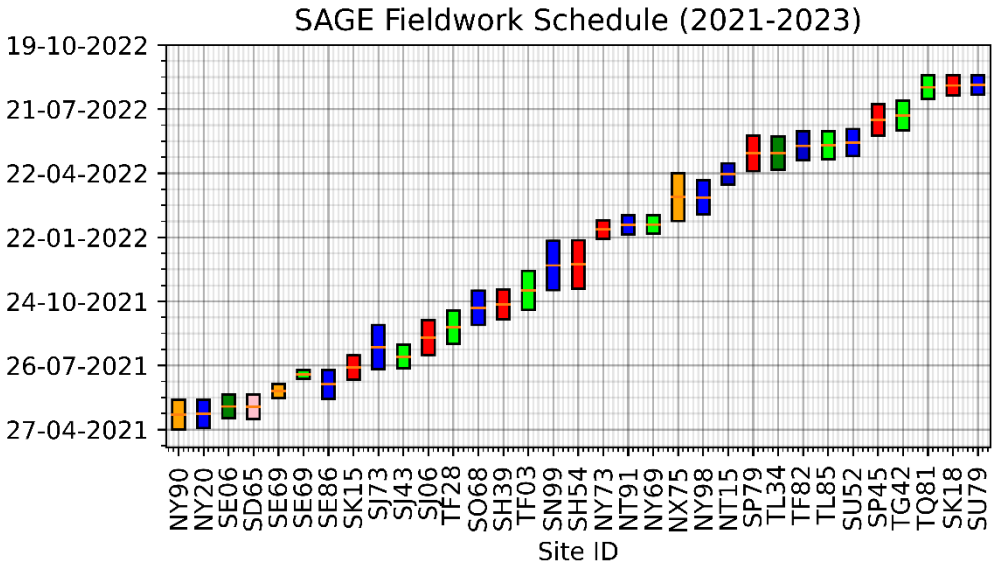

Figure 22: Deployment schedule of all sites up to August 2022. Colours indicate different Lemi system configurations in use.

3.3 DATA COLLECTED APRIL 2021 – JULY 2022

As of August 2022, 32 MT sites have been installed. We chose a naming convention based on Ordnance Survey grid references (Figure 23) with two letters and two numbers. This allows us to incorporate older sites and legacy measurements. The location of MT sites collected so far, as well as those intended for 2022/2023 can be seen in Figure 24.

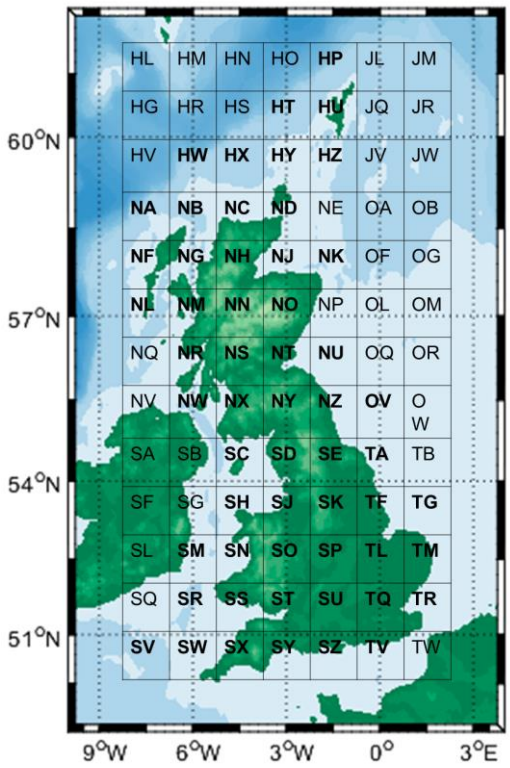

Figure 23: Ordnance Survey Grid reference system provides the naming convention for MT sites.

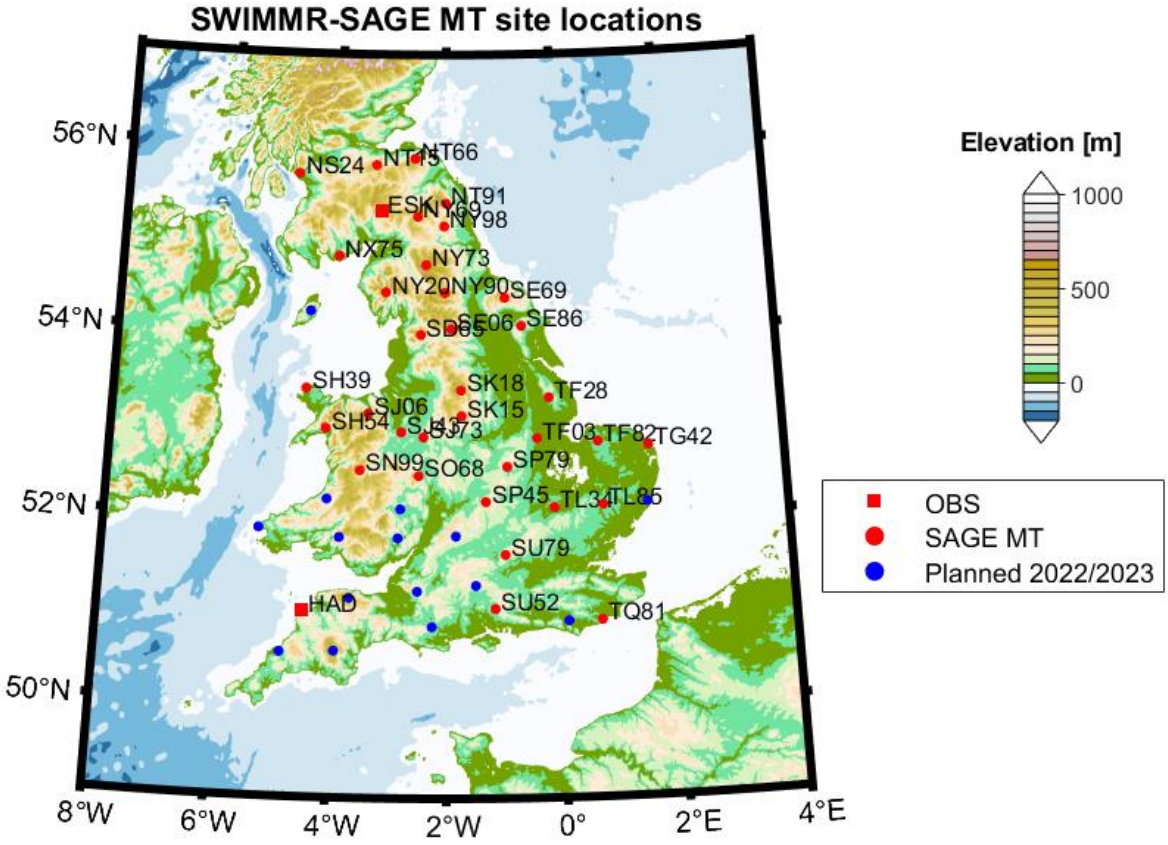

Figure 24: Location of ESK and HAD observatories, SAGE MT sites collected up until July 2022 and planned sites.

Visual inspection of the collected data allows an initial evaluation of data quality. For a high-quality recording, the magnetic and electric fields change smoothly and simultaneously. Rapid changes due to influences from space weather should be correlated between magnetic and electric channels. Figure 25 shows an example from site NY20 in the Lake District, where a small geomagnetic storm was captured on 12 May 2021. Most sites have good data quality, but some suffer from disturbed electric field recordings. This might have been caused by local noise, but also by degradation of the probes (e.g., Figure 26). Some sites have very good electric field data, showing clearly the daily variations and smaller scale changes due to solar influence (Figure 32).

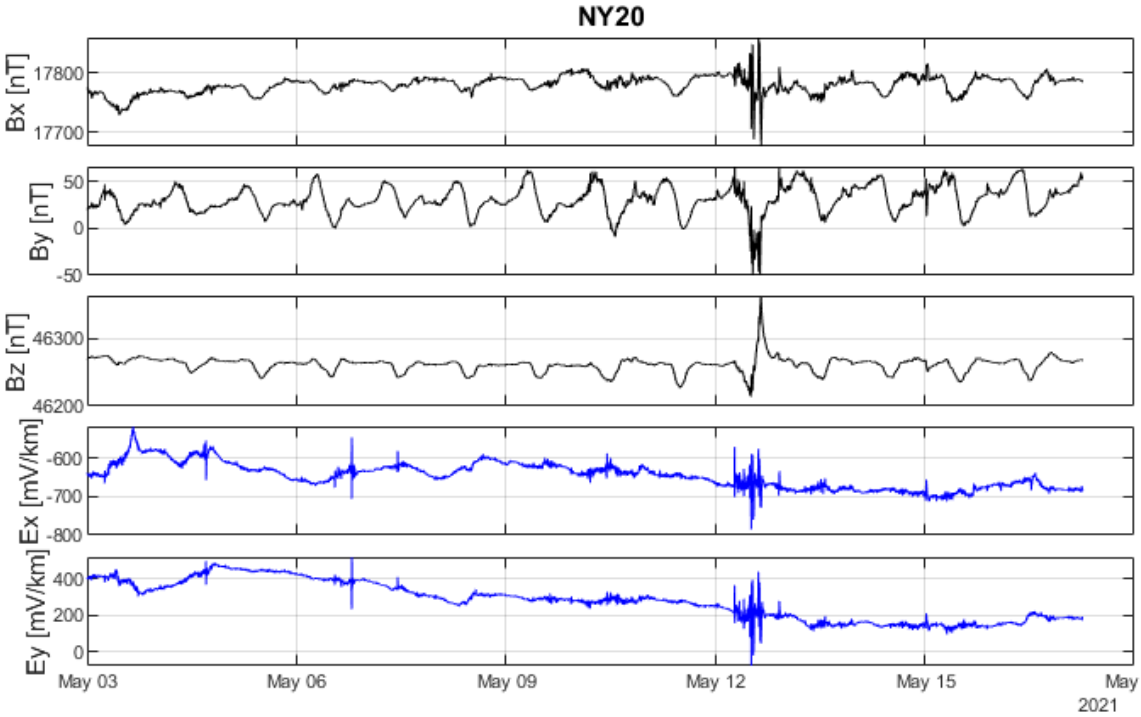

Figure 25: Example of 14 days of timeseries recorded at NY20 (Lake District). Each panel shows one component of the five MT channels (three magnetic and two electric). Daily variations are clearly visible as well as some long-term drift in the electric fields. A minor geomagnetic storm was captured on 12 May 2021.

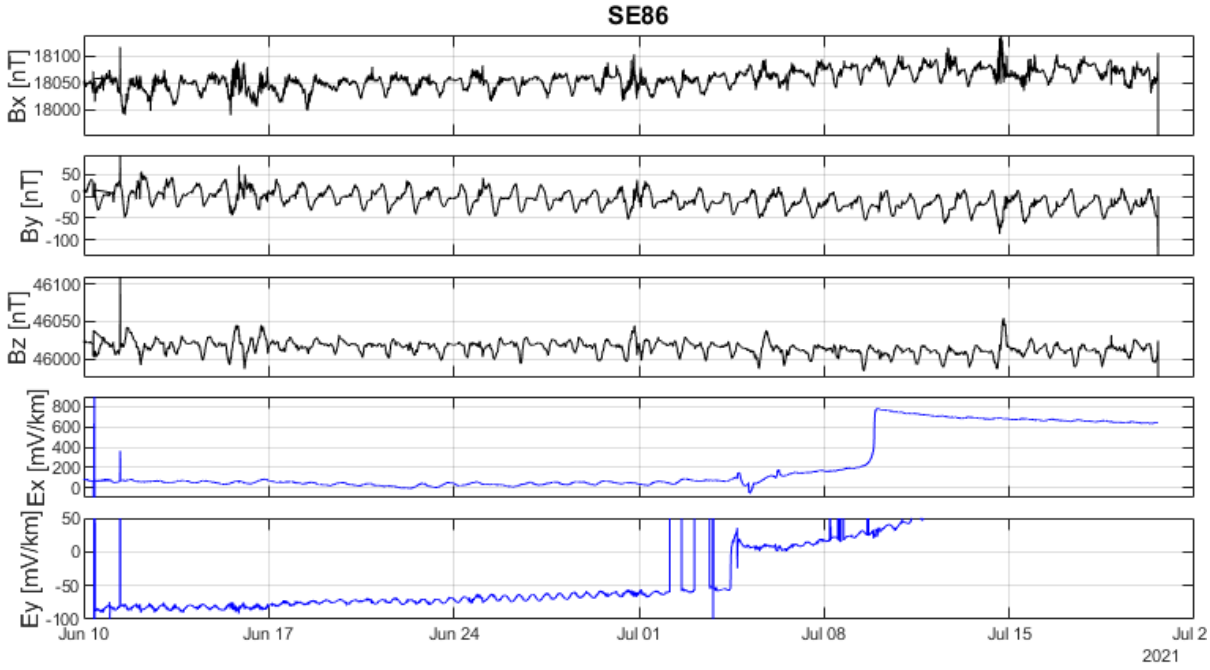

Figure 26: Six weeks long timeseries recorded at SE86 (East Yorkshire) in June-July 2021. Electric fields are relatively clean for the first three weeks and show diurnal variations. In week 4 there is a sudden increase in DC offset which might be due to electrodes drying out.

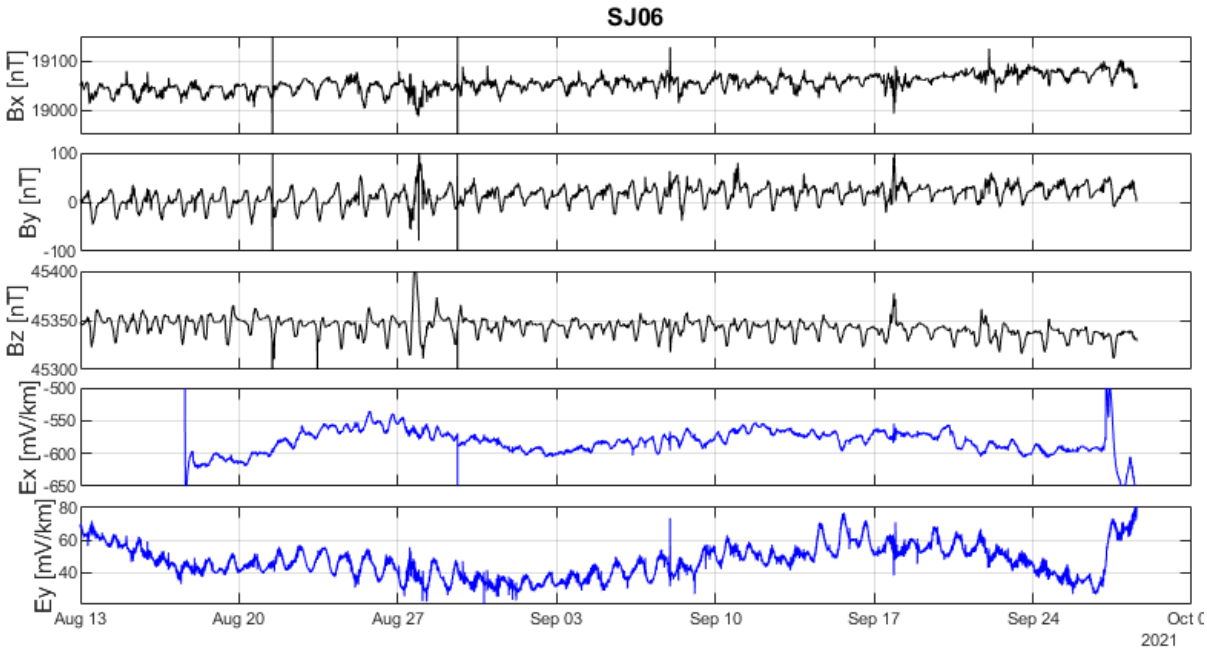

Figure 27: Timeseries recorded at site SJ06 (Malvern). Daily variations (from the ionospheric Sq current) are clearly visible in the electric fields.

3.4 TIME SERIES PROCESSING TO DERIVE MT IMPEDANCE TENSORS

In order to derive the impedance tensor from the timeseries, we used the processing code of Smirnov (2003), which is licenced to the BGS by the author. This software has a user-friendly interface that also allows the fine tuning of the processing parameters that will regulate the impedance estimation. The time series must be corrected for dipole length and system response. A robust estimator finds the optimal impedance estimates and provides information on the uncertainty estimates too.

We also performed comparisons using another freely available software after Egbert (1997) and found that both codes produce very similar results.

The results for 24 sites collected during SAGE are presented in Figure 28, Figure 29 and Figure 30. From visually inspecting the apparent resistivity curves it becomes evident, that the amplitude of the electric field differs vastly across the UK. Local inhomogeneities in the conductivity structures are influencing the MT impedance data by shifting the amplitude of the local electric field. The effect in the data is called galvanic distortion. There will also be local variations that are on a much smaller scale than can be resolved with the density of our measurements.

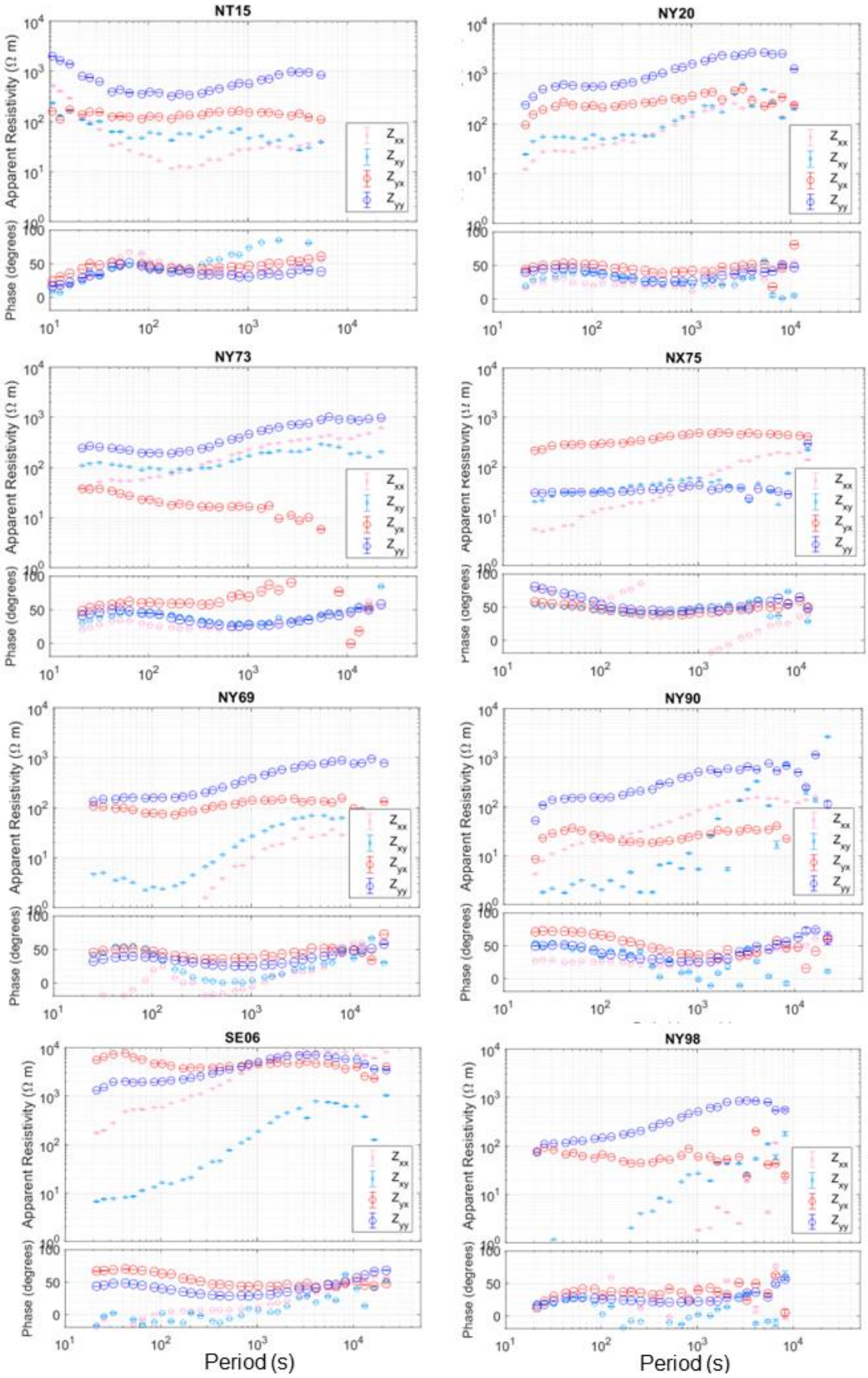

Figure 28: MT impedance tensor estimates for eight SAGE MT sites (NT15. NY20, NY73, NX75, NY69, NY90, SE06, NY98).

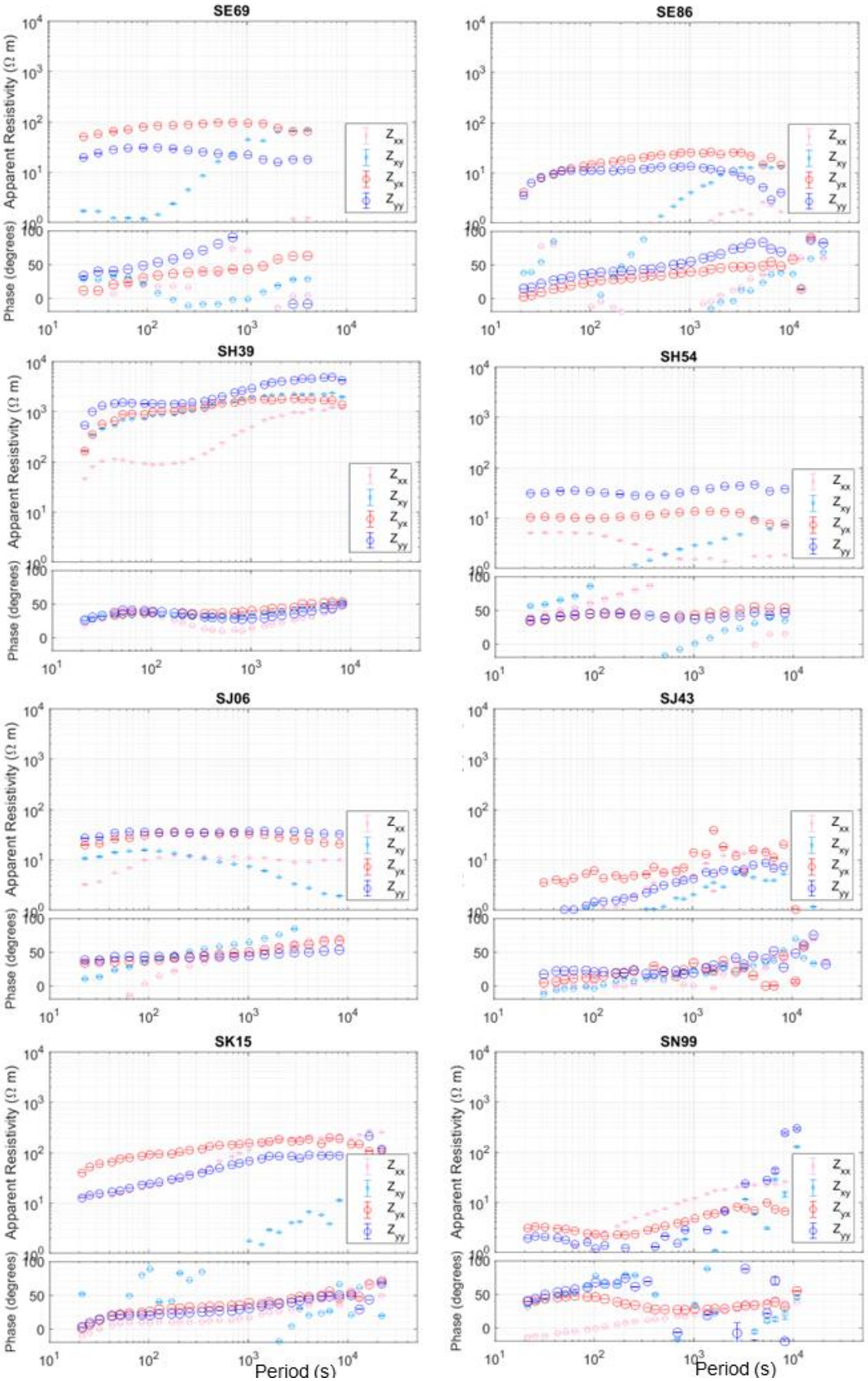

Figure 29: MT impedance tensor estimates for eight SAGE MT sites (SE69, SE86, SH39, SH54, SJ06, SJ43, SK15, SN99).

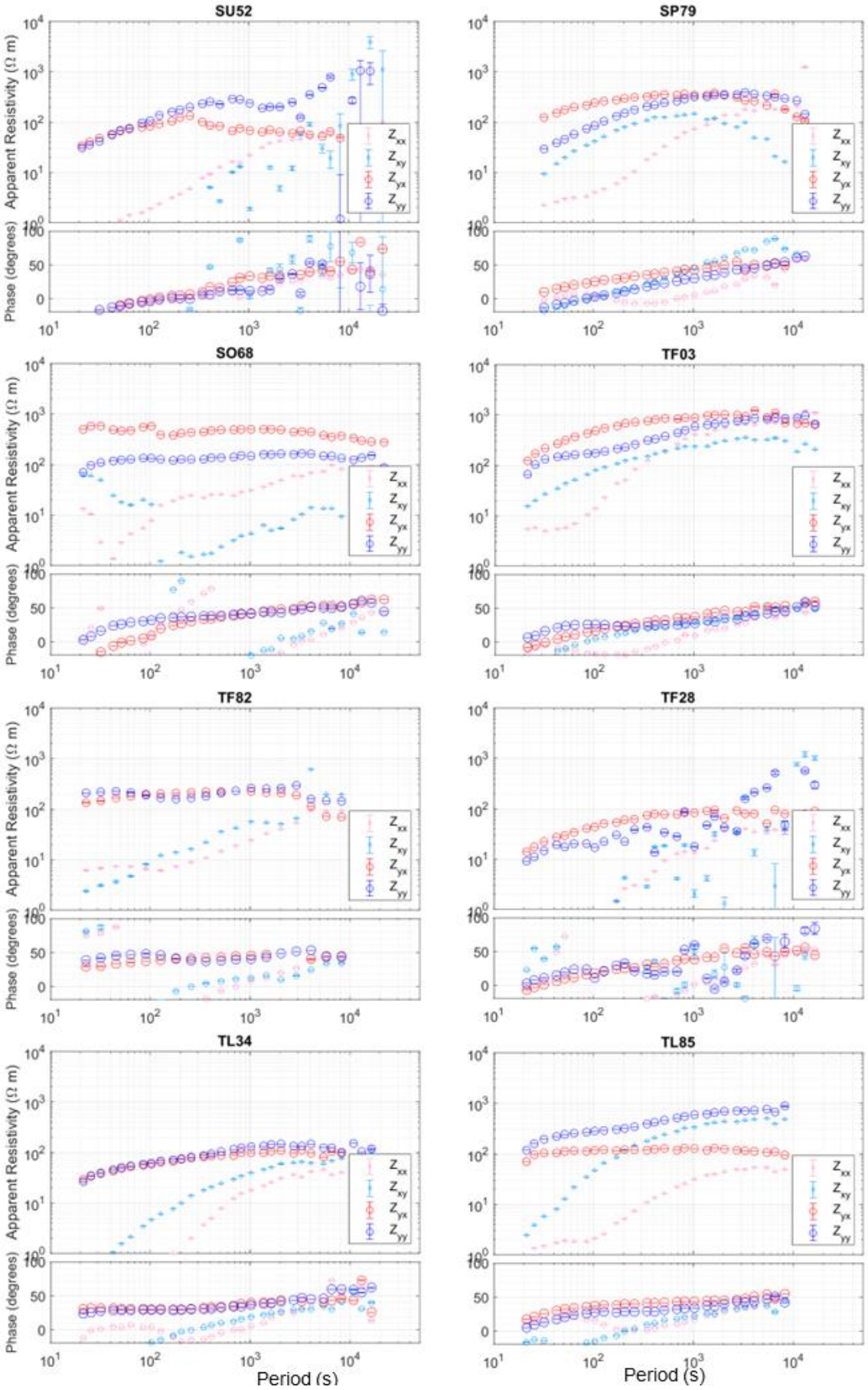

Figure 30: MT impedance tensor estimates for eight SAGE MT sites (SU52, SP79, SO68, TF03, TF82, TF28, TL34, TL85).

3.5 MODELLING GEOELECTRIC FIELDS USING THE NEW MT DATA

With the new MT data set it is now possible to estimate the geoelectric field during geomagnetic storm times over a larger area. Using the algorithm by Campanya *et al.* (2019), as a first study, we calculated the electric field for 33 sites for the September 2017 storm. We used the magnetic field variations measured at 15 sites across the UK, Ireland and western Europe to estimate the ground magnetic field at the MT sites via the Spherical Elementary Current System method (Beggan and Marple, 2018). The magnetic field data are sampled every minute. Modelled electric fields do exceed 200mV/km at several sites in both the Ex and Ey component (see Figure 31) but are much smaller at other locations (Figure 32).

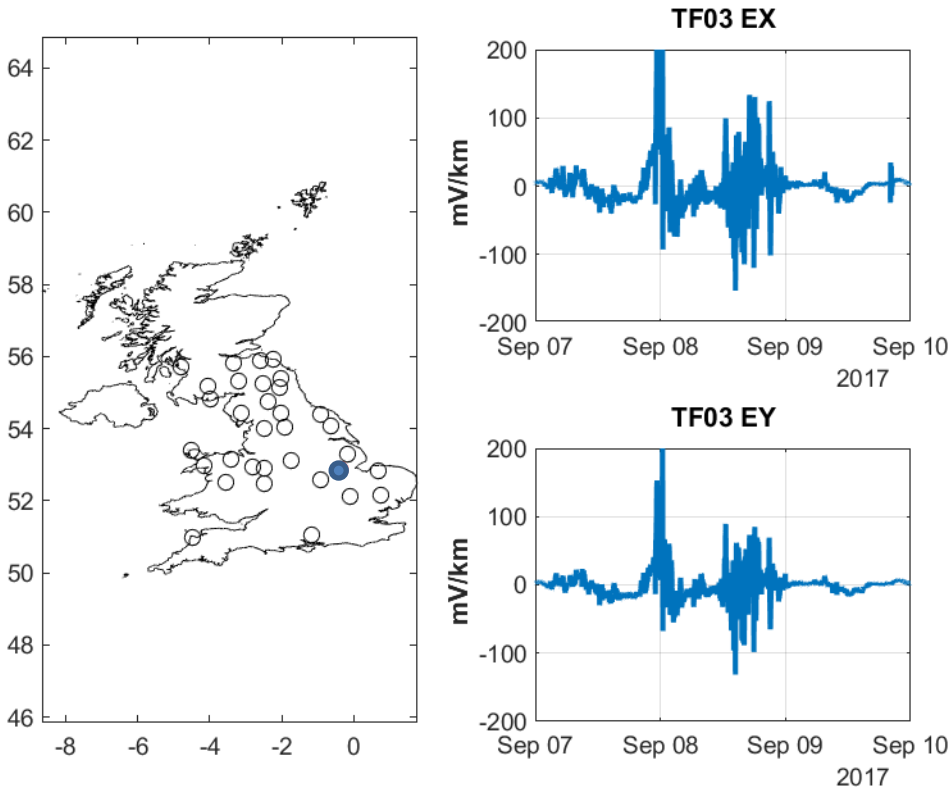

Figure 31: Electric field modelled from MT impedance at site TF03 (Lincolnshire) during the September 2017 storm.

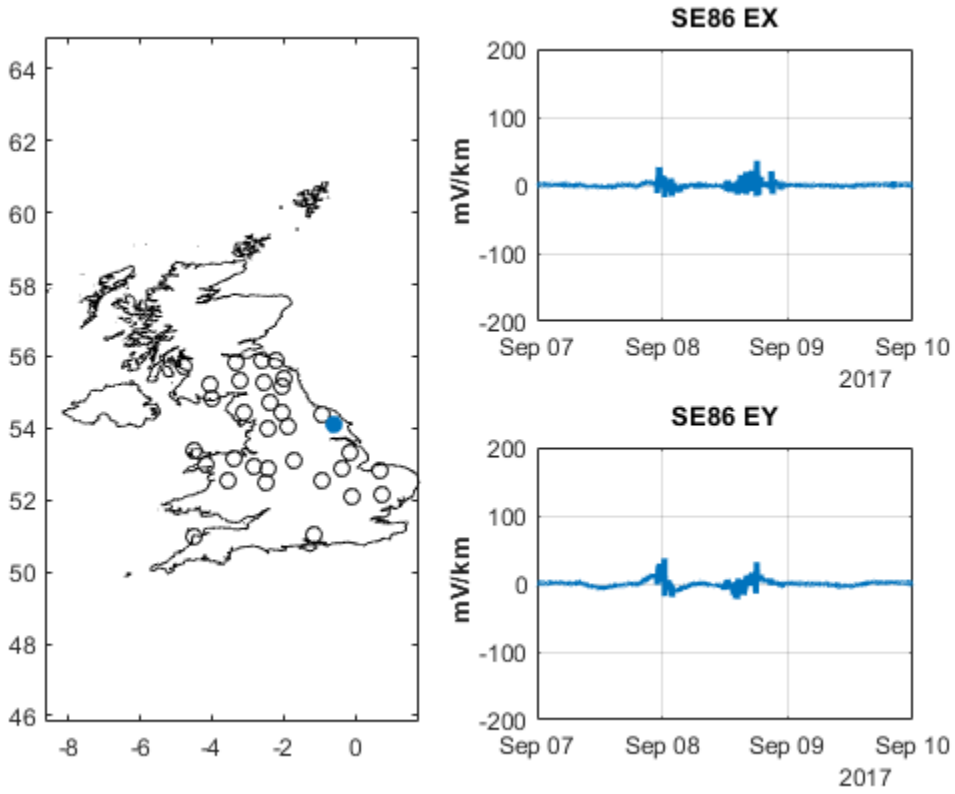

Figure 32: Electric field modelled from MT impedances at site SE86 (Yorkshire) during the September 2017 storm.

Figures 33 and 34 show the modelled electric field estimates at 33 MT sites (29 SAGE sites plus ESK, HAD and two legacy sites in Scotland). We also created maps of the electric field across Britain using two simple interpolation methods (Delaunay triangulation with nearest neighbour and natural). Interpolation between sites will be necessary for the integration of the ground electric field needed for GIC computation. From the interpolated maps we can see that at the most active times there is a north-south trend with decreasing amplitudes with latitude (see especially in the Ey component, in the lower panels of Figures 33 and 34). Apart from this general observation, there are a number of local anomalies, e.g. in south Yorkshire. The derived fields also do not show the coast effect, which is seen in the thin-sheet model. We will be able to study this difference further when the full 3D model is available, which will include a detailed model of the shallow off-coastal sediments.

3.6 MT DATA ACCESS

The MT data collected will be incorporated into the geoelectric field modelling procedures to now- and forecast space weather impacts on grounded infrastructure (the GIC and PSP model). At the end of the project and, after a grace period for the PhD project to publish its findings, the data will be deposited in the NERC Geoscience Data Centre (NGDC) and from there will be openly accessible.

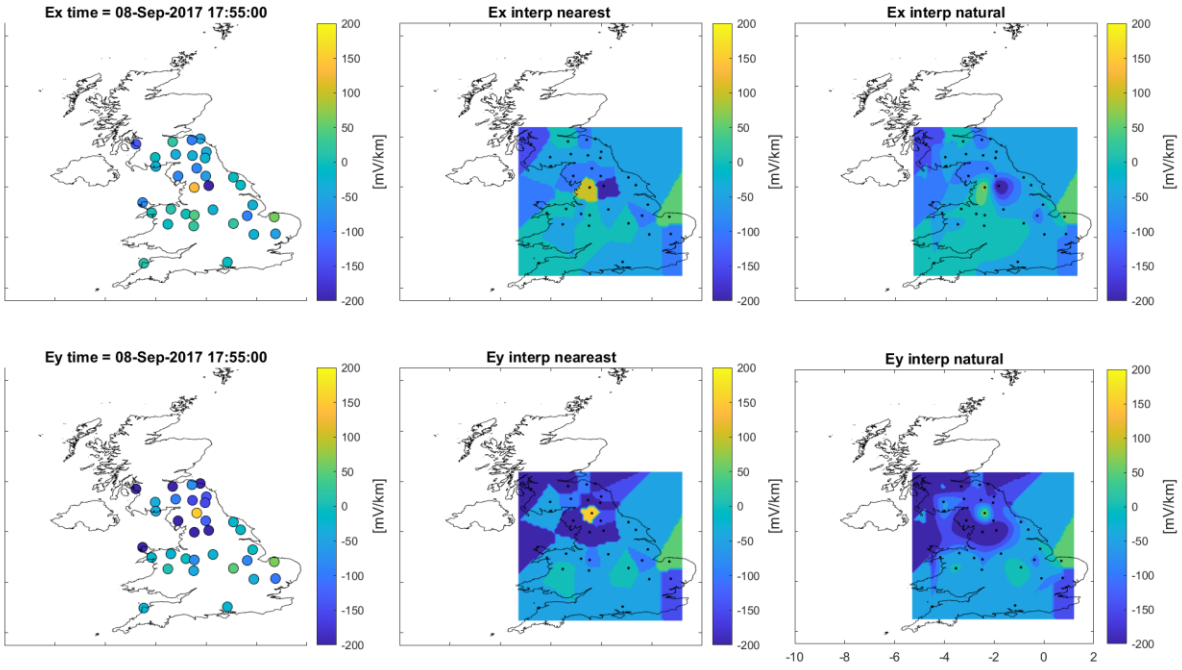

Figure 33: Electric field estimates across field area for 8 Sep 2017, 17:55 (left panels), spatial interpolation using nearest neighbour estimates (middle panel) and natural interpolation (right panels). Note that the time and colour scale are the same as in Figure 16.

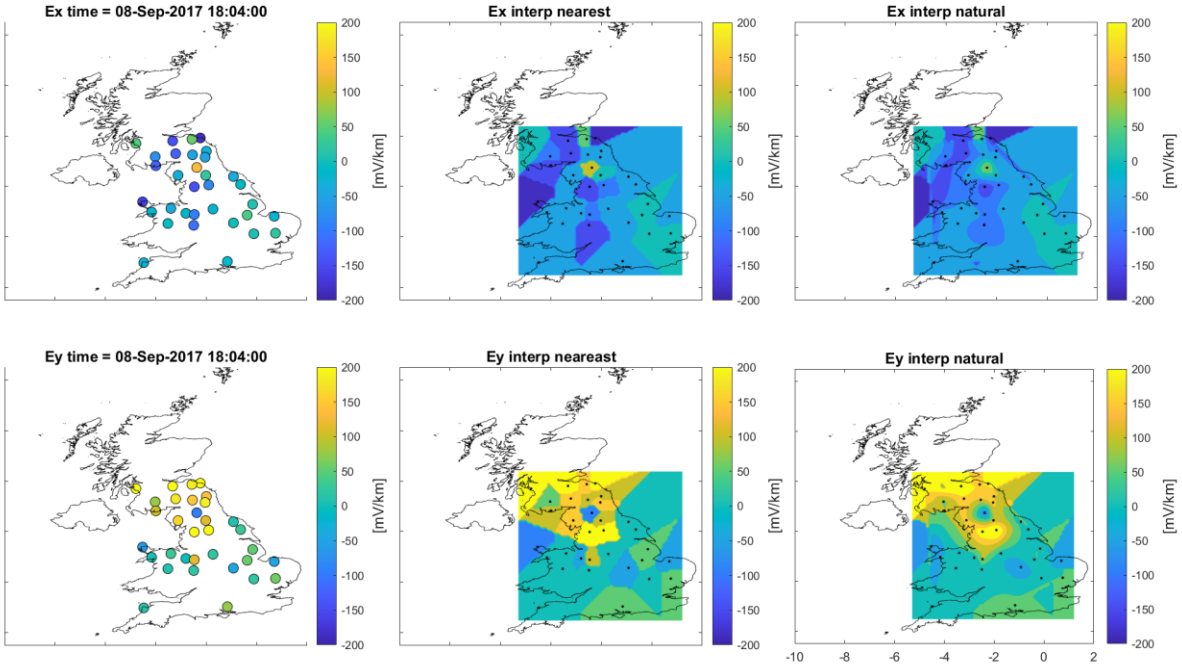

Figure 34: Electric field estimates across the field area for 8 Sep 2017, 18:04 (left panels). Spatial interpolation of the fields using nearest neighbour estimates (middle panel) and natural interpolation (right panels). The timing of this snapshot is the same as in Figure 17.

4 Future work

The results presented in the previous section are the first steps towards a more thorough model of local inhomogeneities in the electric field and from these we can analyse how much they influence the GIC estimates.

4.1 SPATIAL RESOLUTION

After the completion of the fieldwork campaign (March 2023), we will use the new data from southern England and Wales, along with legacy data from Scotland to complete the map of the electric field across Britain. We will investigate the influence of spatial resolution in the dataset (e.g. Murphy *et al.*, 2021) and decrease site spacing where needed, i.e. in areas of strong lateral changes such as in Yorkshire. These can be backfilled over the remainder of the SAGE project (until December 2023).

4.2 3D CONDUCTIVITY MODELLING

After data collection is complete, the PhD project at the University of Edinburgh will focus on inverse modelling of the new MT data set using state-of-the-art parallelized computer algorithms, such as ModEM, which can fully discretise the model space in three dimensions and include onshore topography and offshore bathymetry. Bathymetry is particularly important because the electric currents that flow in salty sea water affect the data at significant distances from the coast. New efforts have been made to better characterize offshore near-coastal sediments and their conductance (*Grayver*, 2021) and we plan to incorporate these into the modelling.

4.3 REAL TIME NOWCASTING AND FORECASTING

At present, the SAGE N4 code for nowcasting and forecasting geoelectric field values from the UK observatories and from the L1 solar wind satellite data streams uses the thin-sheet model and supporting FORTRAN code. As the code is modularised, it is straightforward to replace the geoelectric field code within the Docker-Compose setup on the Amazon Web Services infrastructure.

Figure 35 shows the planned workflow including inputs of data and models to serve the GIC impact nowcast and forecast from SAGE to the Met Office. The box labelled “Thin-sheet model” (central column) will be replaced by the updated “SAGE_MT_map” module. It is envisioned that this new module will consist of the MT impedance functions from the fieldwork campaign and from legacy data in Scotland and will use forward modelling of the magnetic field variation to compute the geoelectric field at each site and then interpolation to produce a 10 x 10 km grid cell map of the geoelectric field for the GIC computation modules. The code will be written and evaluated in Python allowing easier future maintenance.

Beyond the end of the present SAGE project, we envisage the use of the full 3D model of the UK conductivity. A 3D model can be used to predict the ground electric field during space weather events in real-time, for example using the approach developed by Kruglyakov et al., (2022).

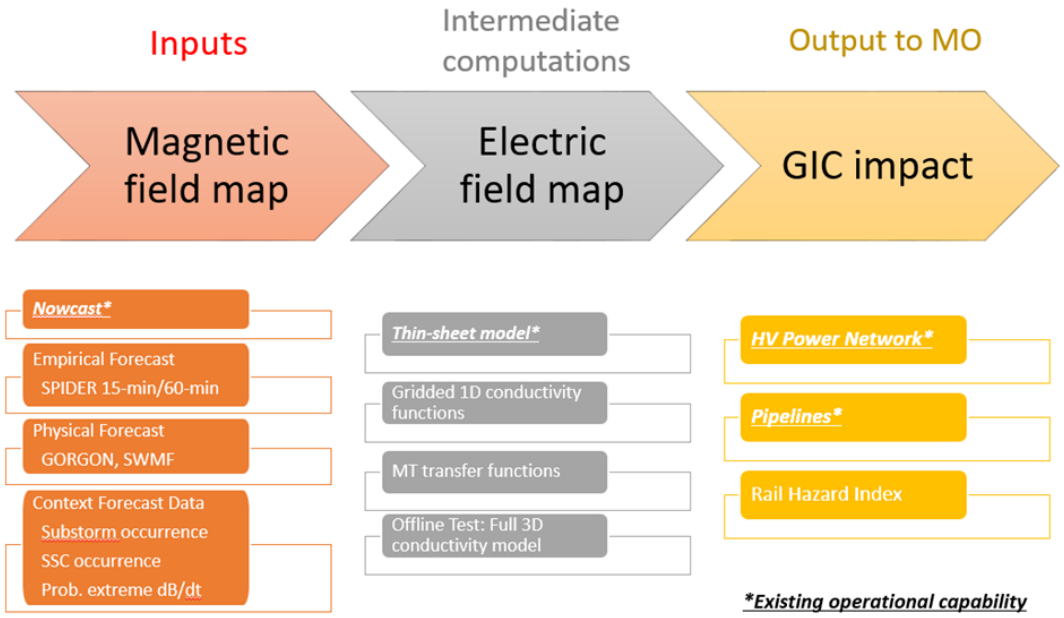

Figure 35: Workflow for SAGE modelling.

Appendix 1

The appendix contains a table with station locations for reference.

Table 1: MT site locations and coordinates in order of deployment.

#	Grid ref	Location	Latitude	Longitude
1	NY90	Richmond	54.44067	-2.026022
2	NY20	Lakes	54.44425	-3.1134318
3	SE06	Appletreewick	54.04938	-1.9106625
4	SD65	Forest of Bowland	53.986667	-2.465556
5	SE69	North Yorkshire moors	54.3846	-0.9251643
6	SE86	Scarborough	54.07972	-0.6292771
7	SK15	Derbyshire	53.11447	-1.7259096
8	SJ73	Market Drayton	52.88483	-2.4068719
9	SJ43	Wrexham	52.93861	-2.8035257
10	SJ06	Denbigh	53.13584	-3.3985801
11	TF28	Lincoln	53.30499	-0.1553931
12	SO68	Shropshire Hills	52.46889	-2.4906282
13	SH39	Anglesey	53.39774	-4.5262569
14	TF03	Grantham	52.86825	-0.3847609
15	SN99	Caersws	52.52497	-3.532127
16	SH54	Porthmadog	52.97288	-4.1587406
17	NY73	Alston	54.74057	-2.375525
18	NT91	Alnham	55.40232	-2.0077226
19	NY69	Kielder Forest	55.25962	-2.5340485
20	NX75	Dumfries	54.83088	-3.9921238
21	NY98	Kirkwhelpington	55.15623	-2.0391719
22	NT15	Nine Mile Burn	55.81058	-3.3223916
23	SP79	Market Harborough	52.56506	-0.9225294
24	TL34	Cambridge	52.1239	-0.1012329
25	TF82	Houghton Hall	52.82396	0.69672383
26	TL85	Shimpling	52.14081	0.75420
27	SU52	Hinton Ampner	51.03599	-1.1563144
28	SP45	Banbury	52.1887	-1.3062458
29	TG42	Long Gores Marsh	52.76779	1.5909811

Glossary

cUK model -3D finite difference representation of the combined thin-sheet conductance and 1D geologic terranes model of the British Isles.

EM induction - Electromagnetic induction, describing the connected effects and interaction of time-varying electric and magnetic fields.

GIC – Geomagnetically induced currents (GICs) are generated from strong ground electric fields during geomagnetic storms.

Ground electric or geoelectric field (GEF) is induced by variations in the magnetic field over a wide frequency/period range. Can be measured with electric dipoles.

Magnetotelluric (MT) method - passive geophysical deep-sounding techniques. MT uses simultaneous measurements of the natural variations in the electric and magnetic field at the Earth's surface to image the conductivity distribution in the subsurface.

Magnetotelluric (MT) impedance tensor – transfer function between horizontal magnetic and electric field changes under a plane-wave assumption. The tensor is frequency dependent and complex.

SWIMMR-SAGE Space Weather Instrumentation, Measurement, Modelling and Risk– Activities in Ground Effects, NERC-STFC programme.

References

AYALA, C., ET AL. (2022), Geomagnetism, Paleomagnetism and Electromagnetism Perspectives on Integrated, Coordinated, Open, Networked (ICON) Science, *Earth and Space Science*, 9(6), e2021EA002141.

AMM, O. (1997), Ionospheric elementary current systems in spherical coordinates and their application, Journal of Geomagnetism and Geoelectricity, Volume 49 (7), page 947-955, 10.5636/jgg.49.947.

BAILLIE, O.. (2020), The Investigating geoelectric tides at three geomagnetic observatories in the UK,.MSCR THESIS, THE UNIVERSITY OF EDINBURGH

BEAMISH, D. (2012), The 1:625k near-surface bedrock electrical conductivity map of the UK, BGS REPORT.

BEAMISH, D., (2013). The bedrock electrical conductivity map of the UK. *Journal of Applied Geophysics*, 96, 87–97. 10.1016/j.jappgeo.2013.06.001

BEGGAN, C.D., (2015) Sensitivity of geomagnetically induced currents to varying auroral electrojet and conductivity models, *Earth, Planets and Space*, 67 (1), 1-12, 10.1186/s40623-014-0168-9

BEGGAN, C. D., G. S. RICHARDSON, O. BAILLIE, J. HÜBERT, AND A. W. P. THOMSON (2021), Geoelectric field measurement, modelling and validation during geomagnetic storms in the UK, *Journal of Space Weather and Space Climate*, 11.

BOLDUC, L., (2002) GIC observations and studies in the Hydro-Québec power system. *J Atmos Sol-Terr Phy.,* 64. 10.1016/S1364-6826(02)00128-1.

BOTELER, D. H., (2006) The super storms of August/September 1859 and their effects on the telegraph system., *Advances in Space Research*, 38(2), 159 – 172. 10.1016/j.asr.2006.01.013

BOTELER, D. H., 2019. A 21st Century View of the March 1989 Magnetic Storm. *Space Weather*, 17, 1–15 10.1029/2019SW002278.

CAMPANYA, J., P. T. GALLAGHER, S. P. BLAKE, M. GIBBS, D. JACKSON, C. D. BEGGAN, G. S. RICHARDSON, AND C. HOGG (2019), Modeling Geoelectric Fields in Ireland and the UK for Space Weather Applications, *Space Weather*, 17(2), 216-237.

EGBERT, G. D. (1997), Robust multiple-station magnetotelluric data processing, *Geophysical Journal International*, 130(2), 475–496-475–496.

GRAYVER, A. V. (2021), Global 3-D Electrical Conductivity Model of the World Ocean and Marine Sediments, *Geochemistry, Geophysics, Geosystems*, 22(9), e2021GC009950.

HÜBERT, J., C. D. BEGGAN, G. S. RICHARDSON, T. MARTYN, AND A. W. P. THOMSON (2020), Differential Magnetometer Measurements of Geomagnetically Induced Currents in a Complex High Voltage Network, *Space Weather*, 18(4), e2019SW002421.

KELBERT, A. (2020), The Role of Global/Regional Earth Conductivity Models in Natural Geomagnetic Hazard Mitigation, *Surveys in Geophysics*, 41(1), 115-166.

JANKOWSKI, J. SUCKSDORFF, C. (1996), The IAGA guide for magnetic measurements and observatory practice, *International Association of Geomagnetism and Aeronomy*

KELBERT, A., N. MEQBEL, G. D. EGBERT, AND K. TANDON (2014), ModEM: A modular system for inversion of electromagnetic geophysical data, *COMPUTERS & GEOSCIENCES*, 66, 40-53.

KRUGLYAKOV, M., A. KUVSHINOV, AND E. MARSHALKO (2022), Real-Time 3-D Modeling of the Ground Electric Field Due To Space Weather Events. A Concept and Its Validation, *Space Weather*, 20(4).

LOVE, J. J., G. M. LUCAS, A. KELBERT, and P. A. BEDROSIAN, (2018) Geoelectric Hazard Maps for the Mid-Atlantic United States: 100 Year Extreme Values and the 1989 Magnetic Storm. *Geophysical Research Letters*, 45(1), 5–14. 10.1002/2017GL076042

LUCAS, G. M., J. J. LOVE, AND A. KELBERT (2018), Calculation of Voltages in Electric Power Transmission Lines During Historic Geomagnetic Storms: An Investigation Using Realistic Earth Impedances, *Space Weather*, 16(2), 185-195.

MCKAY, A. (2003), Geoelectric fields and Geomagnetically Induced Currents in the United Kingdom. Ph.D. thesis, University of Edinburgh. http://hdl.handle.net/1842/639.

MURPHY, B. S., G. M. LUCAS, J. J. LOVE, A. KELBERT, P. A. BEDROSIAN, AND E. J. RIGLER (2021), Magnetotelluric Sampling and Geoelectric Hazard Estimation: Are National-Scale Surveys Sufficient?, *Space Weather*, 19(7).

OUGHTON, E. J., M. HAPGOOD, G. S. RICHARDSON, C. D. BEGGAN, A. W. P. THOMSON, ET AL. (2018), A Risk Assessment Framework for the Socioeconomic Impacts of Electricity Transmission Infrastructure Failure Due to Space Weather: An Application to the United Kingdom. *Risk Analysis*, 38(12), 1–22 10.1111/risa.13229

PULKKINEN, A., E. BERNABEU, J. EICHNER, C. BEGGAN, and A. THOMSON (2012), Generation of 100-year geomagnetically induced current scenarios. *Space Weathe*r, 10, S04,003. 10.1029/2011SW000750.

ROGERS, N. C., J. A. WILD, E. F. EASTOE, J. W. GJERLOEV, and A. W. P. THOMSON (2020), A global climatological model of extreme geomagnetic field fluctuations. *J. Space Weather Space Clim*., 10, 5, 10.1051/swsc/2020008

ROSENQVIST, L., T. FRISTEDT, A. P. DIMMOCK, P. DAVIDSSON, R. FRIDSTRÖM, ET AL. (2022), 3D Modeling of Geomagnetically Induced Currents in Sweden — Validation and Extreme Event Analysis. *Space Weather*,20(3), e2021SW002,988. 10.1029/2021SW002988.

SIMPSON, F., and K. BAHR (2021), Nowcasting and validating Earth's electric-field response to extreme space-weather events using magnetotelluric data: application to the September 2017 geomagnetic storm and comparison to observed and modelled fields in Scotland. *Space Weather*, 19, e2019SW002,432, 10.1029/2019SW002432

SMIRNOV, M. Y. (2003), Magnetotelluric data processing with a robust statistical procedure having a high breakdown point, *Geophysical Journal International*, 152(1), 1-7.

Smirnov, M. (2008), Magnetotelluric data processing with a robust statistical procedure having a high breakdown point. *Geophysical Journal International*, 152(1), 1–7. 10.1046/j.1365-246X.2003.01733.x.

TAUBER, S., R. BANKS, O. RITTER, U. WECKMANN, AND A. JUNGE (2003), A high-resolution magnetotelluric survey of the Iapetus Suture Zone in southwest Scotland, *Geophysical Journal International,* 153(3), 548-568.

THOMSON, A. W. P., E. DAWSON, and S. REAY (2011), Geomagnetic Extreme Statistics for Europe. *Space Weather*, 9, S10,001. 10.1029/2011SW000696

VASSEUR, G., AND P. WEIDELT (1977), Bimodal electromagnetic induction in non-uniform thin sheets with an application to the northern Pyrenean induction anomaly, *Geophys. J. R. Astr*. SOC., 51, 669-690.